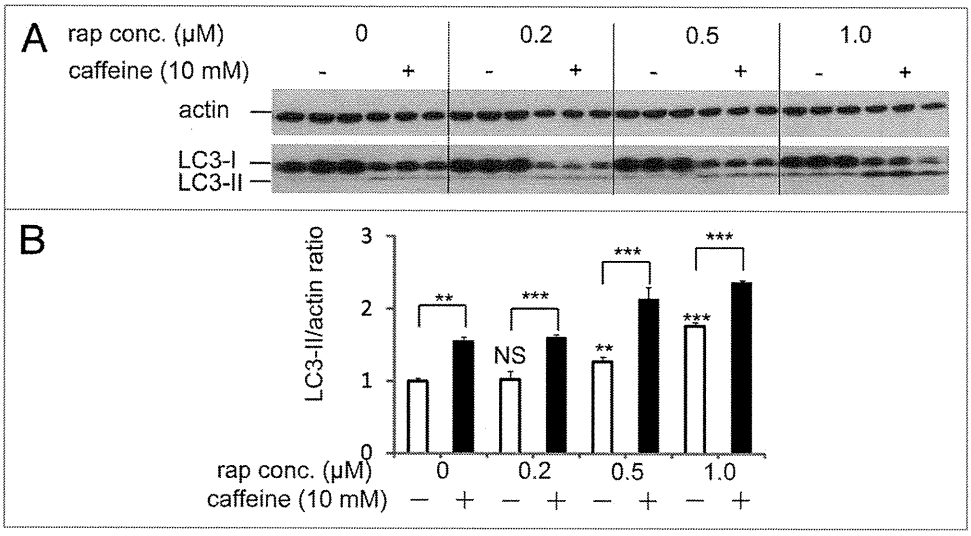

Figure 5. Rapamycin treatment with caffeine has an additive effect on enhancement of autophagy. (A) SH-SY5Y cells treated with various concentrations of rapamycin with or without 10 mM caffeine for 48 hours were analyzed by immunoblotting. (B) Densitometry analysis was performed using three independent experiments. Error bars, SD; *p < 0.05; **p < 0.01; N.S., not significant.

intervention strategy for the upregulation of apoptosis by a harnessing of its autophagic activity in tumor treatment.

Materials and Methods

Cell line. HeLa cells were maintained in DMEM (Sigma) supplemented with 10% fetal bovine serum (FBS) (Sigma) and 100 U/ml penicillin/streptomycin (Sigma) at 37°C and 5% CO_2. PC12D and SH-SY5Y cells were maintained in DMEM (Sigma) supplemented with 10% FBS (Sigma), 5% horse serum and 100 U/ml penicillin/streptomycin at 37°C and 5% CO_2. All experiments with PC12D were performed after differentiation with NGF treatment for 48 hours. $Atg7^{+/+}$ and $^{-/-}$ MEFs were maintained in DMEM (Sigma) supplemented with 10% FBS, 100 U/ml penicillin/streptomycin, 1% sodium pyruvate (Gibco, 11360), 1% non-essential amino acid (NEAA) and 4.2 μl 2% beta-mercaptoethanol at 37°C.

To establish a HeLa GFP-LC3 stable cell line, proliferating HeLa cells were transfected with a GFP-LC3 plasmid.[14] Forty-eight hours post-transfection with Lipofectamine 2000 (Invitrogen), positive stable clones were selected by growing cells with G418 (400 μg/ml) for 2 weeks and maintained in DMEM (Sigma) supplemented with 10% FBS (Sigma), 100 U/ml penicillin/streptomycin and 200 μg/ml G418 at 37°C and 5% CO_2. All cellular experiments were performed with cells cultured in complete medium with FBS as explained above.

Cell viability assays. A trypan blue dye (Invitrogen, 15250-061) exclusion assay was used to examine cell viability and performed according to previously reported protocols.[40,41] Changes of mitochondrial membrane potentials were assessed also with the lipophilic cationic membrane potential-sensitive dye JC-1 (5,5',6,6'-tetrachloro-1,1',3,3'-tetraethylbenzimidazolylcarbocyanineiodide) (Wako, 106-00131) according to the manufacturer's protocol. Detection of early apoptotic cells was determined using an annexin V/propidium iodide (PI) detection kit (Invitrogen), according to the manufacturer's protocol. Briefly, 0.5 x 10^6 $Atg7^{+/+}$ or $^{-/-}$ MEFs were exposed to caffeine (0–25 mM) for 24 hours and washed twice. Then, they were incubated at room temperature with annexin V/Alexa488 and PI for 15 minutes. Annexin V^+PI^- cells, considered as early apoptotic cells, were enumerated using FACScan (BD Biosciences). Data were analyzed with CellQuest (BD Biosciences) and FlowJo softwares (Tree Star Inc.). Cells positive or negative for annexin V were regarded as apoptotic or non-apoptotic cells, respectively.

Cell cycle analysis. To examine apoptosis, 1.0 x 10^4 cells/well PC12D cells were seeded onto 96-well culture plate and incubated for 48 h in DMEM with NGF and treated with caffeine for 72 h. The cells were harvested and washed with PBS and

Figure 6 (See opposite page). Caffeine induces apoptosis by enhancement of autophagy. (A) After PC12D cells were treated with 0, 1, 2.5, 5 or 10 mM caffeine with DMSO or MPP^+ for 72 hours, cell viability was measured using trypan blue dye exclusion assay. Data are the means of triplicate experiments. (B) After cells were treated with 0, 1, 2.5, 5 or 10 mM caffeine with DMSO or MPP^+ for 48 hours, mitochondrial membrane potential was analyzed by JC-1 using a flow cytometry. Data are the means of triplicate experiments. (C) After PC12D cells were treated with 0, 1, 2.5, 5 or 10 mM caffeine with DMSO or MPP^+ for 72 hours, caffeine-induced sub G_1 area was analyzed by propidium iodide staining assay using a flow cytometry. Data are the means of triplicate experiments. (D) PC12D cells were treated with H_2O or caffeine for 24 hours or staurosporine (positive control) for 3 hours and analyzed with immunoblotting for levels of caspase-3 and cleaved caspase-3. (E) After PC12D cells were treated with 0, 1, 2.5, 5 or 10 mM caffeine with or without 1, 3 or 5 mM 3MA for 24 hours, cell viability was measured by trypan blue dye exclusion assay. (F) PC12D cells were transfected with control siRNA or siRNAs targeting Atg7. Forty eight hours later, they were treated with 0, 1, 2.5 or 10 mM caffeine for 24 hours and mitochondrial membrane potential was analyzed using JC-1. The knockdown effects on Atg7 were confirmed by immunoblotting using antibodies against Atg7 and actin. Data are the means of triplicate experiments. Error bars, S.D. NS, not significant; *p < 0.05; **p < 0.01; ***p < 0.001.

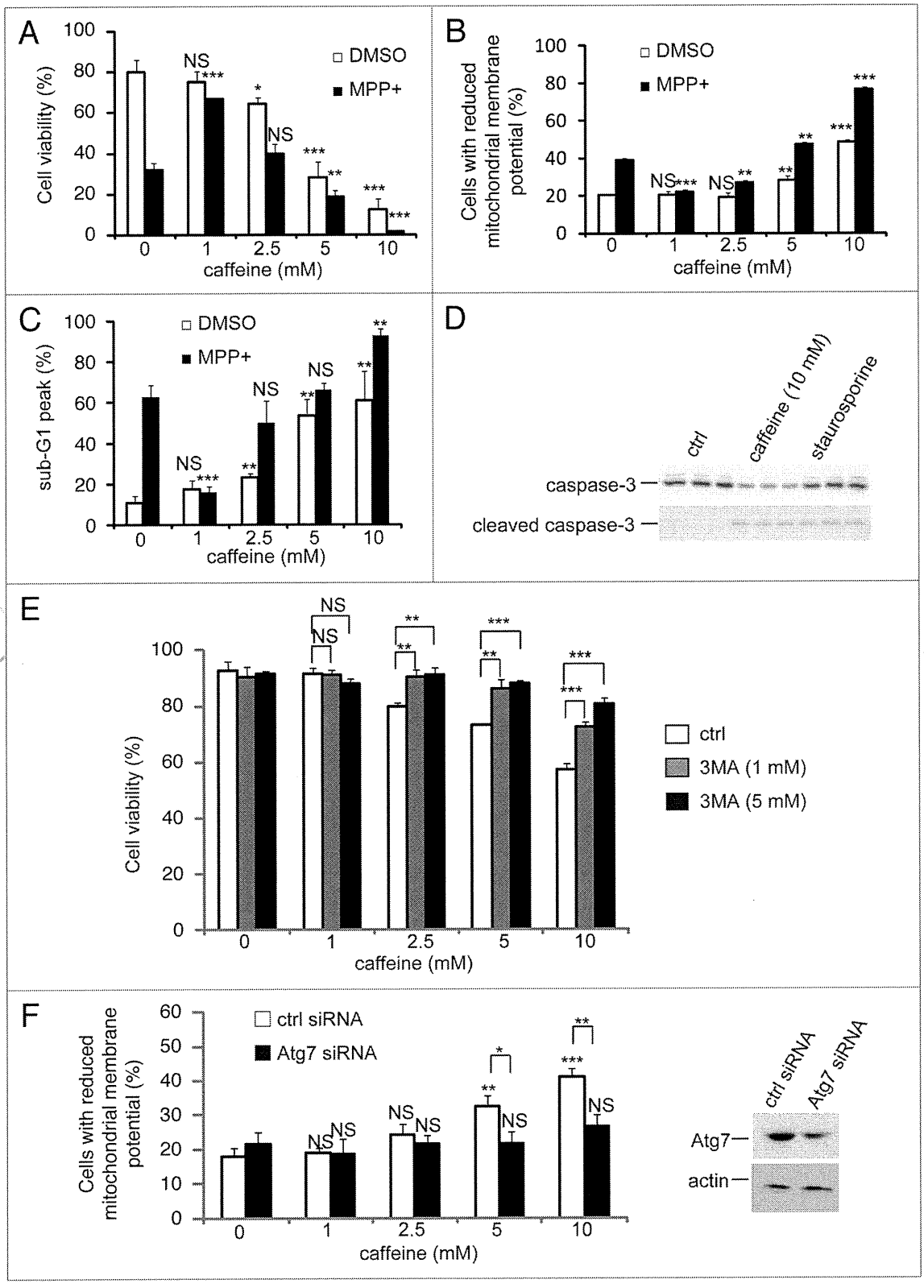

fixed with ice-cold 70% ethanol at 4°C for 2 h. The cells were then stained with PI solution according to previously reported protocol.[41] DNA content was analyzed by flow cytometry using FACScan and CellQuest software (BD Biosciences).

Compounds. Compounds used included caffeine (Wako, 031-06792), E64d (Sigma, E8640), pepstatin A (Sigma, P5318), rapamycin (LC Laboratories, R5000), CCI-779 (Selleck Chemicals, S1044), MPP+ (Sigma, M0896), bafilomycin A1 (Sigma, B1793), 3-methyladenine (Sigma, M9281), insulin (Sigma, I0516), U0126 (Sigma, U120), Akt1/2 inhibitors (Sigma, A6730), staurosporine (Cell Signaling Technology, 9953) and DMSO (Sigma, D2650).

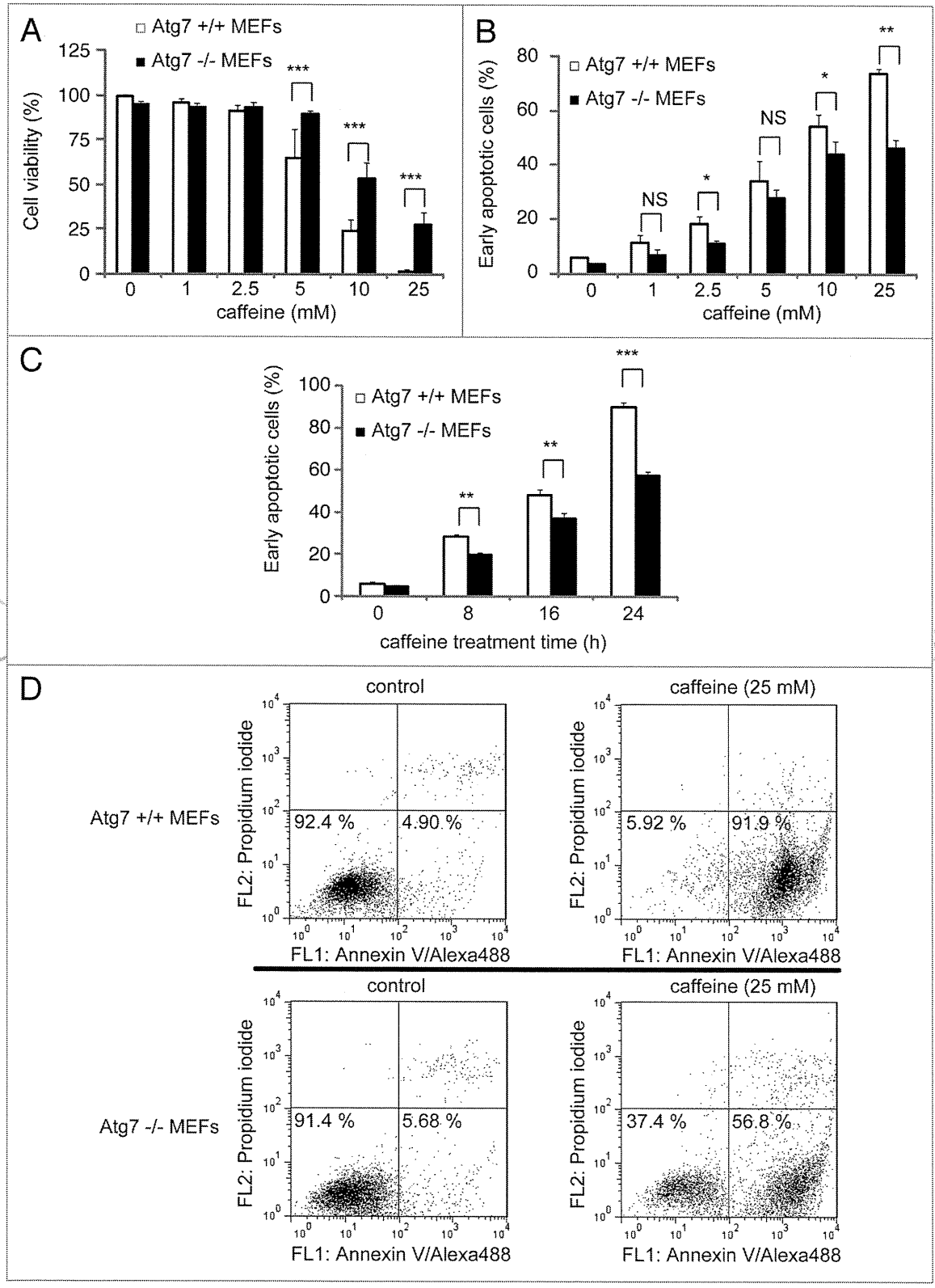

Figure 7. Cells without Atg7 expression are more resistant to caffeine-induced apoptosis. (A) After Atg7$^{+/+}$ or $^{-/-}$ mouse embryonic fibroblasts (MEFs) were treated with 0, 1, 2.5, 5, 10, 25 mM caffeine for 24 hours, the cell viability was measured by trypan blue dye exclusion assay. Data are the means of triplicate experiments. (B–D) Fluorescence-activated cell-sorting analysis for annexin V/propidium iodide (PI). Atg7$^{+/+}$ or $^{-/-}$ MEFs were cultured with various concentrations of caffeine for 24 hours (B) or with 25 mM caffeine for various times (0, 8, 16 or 24 hours) (C and D). Annexin V/PI staining was subsequently performed to assess early or late apoptosis and necrosis. 5 x 10^3 cells were analyzed by flow cytometry and the percentage of early apoptotic cells (annexin V-positive and PI-negative cells, the lower right region in (D) was determined). Data are the means of triplicate experiments. Error bars, SD. NS, not significant; *$p < 0.05$; **$p < 0.01$; ***$p < 0.001$.

Plasmid DNAs. Myrystoylated Akt (21–151), a constitutively active form of Akt, was purchased from Millipore.

siRNA knockdown experiments. PC12D cells were transfected with rat Atg7 siRNAs (Invitrogen, 10620318-9) using Lipofectamine RNAiMAX (Invitrogen, 13778-075) according to the manufacturer's protocol.

Western blotting. Cell pellets were lysed on ice in RIPA buffer for 20 minutes in the presence of protease inhibitor (Roche). Western blotting was performed according to a previously published report.[42] The antibodies used were as follows: anti-p70 ribosomal protein (Cell Signaling Technology, 2708), anti-ribosomal protein (Cell Signaling Technology, 2217), anti-4E-BP1 (Cell Signaling Technology, 9452), anti-Akt (Cell Signaling Technology, 9272), anti-p44/42 MAP kinase (Cell Signaling Technology, 9102), anti-phospho-p70 ribosomal protein (Thr389) (Cell Signaling Technology, 9205), anti-phospho-S6 ribosomal protein (Ser235/236) (Cell Signaling Technology, 2211), anti-phospho-4E-BP1 (Thr37/46) (Cell Signaling Technology, 9459), anti-phospho-p44/p42 MAPK (Thy202/Tyr204) (Cell Signaling Technology, 9101), anti-Atg7 (Cell Signaling Technology, 2631), anti-phospho-Akt (Cell Signaling Technology, 4060), anti-actin (Millipore, clone C4), anti-LC3 (MBL, clone 4E12), anti-p62 (Progen Biotechnik, GP62-C) antibodies. Antibody signals were enhanced with chemifluorescent methods from GE HealthCare.

Immunofluorescent microscopy. Cells were embedded with 4% paraformaldehyde for 20 minutes. Following this, they were permeabilized with 0.1% Triton-X in 1x PBS. After incubation with 10% FBS and 1% bovine serum albumin in 1x PBS for 30 minutes, cells were immunostained with anti-LC3B (x500) (Sigma, L7543), anti-LAMP2 (x50) (Development Studies Hybridoma Bank, clone H4B4) overnight and incubated with anti-rabbit IgG tagged with AlexaFluor 488 or anti-mouse IgG tagged with AlexaFluor 546 for 1 hour. The cover slips were embedded with VectaShield, stained with DAPI and images were acquired on a Zeiss LSM510 META confocal microscope (63 x 1.4 NA) or a Leica TCS SP5 confocal microscope at room temperature using Zeiss LSM510 v.3.2 software or Leica LAS AF software. Adobe Photoshop 7.0 (Adobe Systems Inc.) was used for subsequent image processing. For colocalization assay in HeLa cells, an appropriate confocal image was taken with Leica LAS AF software. Then, these images were analyzed automatically with the ImageJ "Colocalization" Plugin (Settings: Each threshold: 25, Ratio: 75%) followed by "Analyze particles" (Settings: threshold 25; Pixel: 1) between endogenous LC3 positive and LAMP2 vesicles. Experiments were done in triplicate at least twice.

Quantification of cells with GFP-LC3 vesicles. HeLa cells stable expressing GFP-LC3 were treated with various concentrations of caffeine for 24 or 48 hours and then fixed as described above. Analyses in triplicate were done for counting the proportion of GFP-positive cells with GFP-LC3 vesicles as previously described in reference 43.

Electron microscopy. SH-SY5Y cells treated with various concentrations of caffeine were prefixed in 2% glutaraldehyde in PBS at 4°C, treated with 1% OsO_4 for 3 hours at 4°C, dehydrated in a graded series of ethanol and flat embedded in epon. Ultra-thin sections were doubly stained with uranyl acetate and observed using a JEOL JEM-2000EX electron microscopy at 80 kV.

Statistical analysis. Densitometry analysis was performed using ImageJ 1.43 on immunoblots from three independent experiments. A t-test was performed with SYSTAT software (Hulinks).

Acknowledgements

We thank Dr. Takashi Ueno (Department of Biochemistry, Juntendo University) for critical comments and Drs. Masaaki Komatsu and Yu-Shin Sou for providing Atg7$^{+/+}$ and $^{-/-}$ MEFs. We are very grateful for a grant from Hayashi Memorial Foundation for Female Natural Scientists (Y.S.), the Grant-in-Aid for Young Scientists (B) (S. Saiki and F. Sato), grants from the All Japan Coffee Association (S. Saiki), the Takeda Scientific Foundation (S. Saiki) and the Nagao Memorial Fund (S. Saiki).

Note

Supplementary materials can be found at:
www.landesbioscience.com/supplement/SaikiAUTO7-2-Sup.pdf

References

1. Bode AM, Dong Z. The enigmatic effects of caffeine in cell cycle and cancer. Cancer Lett 2007; 247:26-39.
2. Jang MH, Shin MC, Kang IS, Baik HH, Cho YH, Chu JP, et al. Caffeine induces apoptosis in human neuroblastoma cell line SK-N-MC. J Korean Med Sci 2002; 17:674-8.
3. Gururajanna B, Al-Katib AA, Li YW, Aranha O, Vaitkevicius VK, Sarkar FH. Molecular effects of taxol and caffeine on pancreatic cancer cells. Int J Mol Med 1999; 4:501-7.
4. Qi W, Qiao D, Martinez JD. Caffeine induces TP53-independent G(1)-phase arrest and apoptosis in human lung tumor cells in a dose-dependent manner. Radiat Res 2002; 157:166-74.
5. Mizushima N, Levine B, Cuervo AM, Klionsky DJ. Autophagy fights disease through cellular self-digestion. Nature 2008; 451:1069-75.
6. Rubinsztein DC. The roles of intracellular protein-degradation pathways in neurodegeneration. Nature 2006; 443:780-6.
7. Eisenberg-Lerner A, Bialik S, Simon HU, Kimchi A. Life and death partners: apoptosis, autophagy and the cross-talk between them. Cell Death Differ 2009; 16:966-75.
8. Espert L, Denizot M, Grimaldi M, Robert-Hebmann V, Gay B, Varbanov M, et al. Autophagy is involved in T cell death after binding of HIV-1 envelope proteins to CXCR4. J Clin Invest 2006; 116:2161-72.
9. Foukas LC, Daniele N, Ktori C, Anderson KE, Jensen J, Shepherd PR. Direct effects of caffeine and theophylline on p110delta and other phosphoinositide 3-kinases. Differential effects on lipid kinase and protein kinase activities. J Biol Chem 2002; 277:37124-30.
10. Kudchodkar SB, Yu Y, Maguire TG, Alwine JC. Human cytomegalovirus infection alters the substrate specificities and rapamycin sensitivities of raptor- and rictor-containing complexes. Proc Natl Acad Sci USA 2006; 103:14182-7.
11. Winter G, Hazan R, Bakalinsky AT, Abeliovich H. Caffeine induces macroautophagy and confers a cytocidal effect on food spoilage yeast in combination with benzoic acid. Autophagy 2008; 4:28-36.
12. Rubinsztein DC, Cuervo AM, Ravikumar B, Sarkar S, Korolchuk V, Kaushik S, Klionsky DJ. In search of an "autophagomometer". Autophagy 2009; 5:585-9.
13. Tanida I, Ueno T, Kominami E. LC3 and Autophagy. Methods Mol Biol 2008; 445:77-88.
14. Kabeya Y, Mizushima N, Ueno T, Yamamoto A, Kirisako T, Noda T, et al. LC3, a mammalian homologue of yeast Apg8p, is localized in autophagosome membranes after processing. EMBO J 2000; 19:5720-8.
15. Yamamoto A, Tagawa Y, Yoshimori T, Moriyama Y, Masaki R, Tashiro Y. Bafilomycin A1 prevents maturation of autophagic vacuoles by inhibiting fusion between autophagosomes and lysosomes in rat hepatoma cell line, H-4-II-E cells. Cell Struct Funct 1998; 23:33-42.
16. Mizushima N, Yoshimori T, Levine B. Methods in mammalian autophagy research. Cell 140:313-26.
17. Hanahan D, Weinberg RA. The hallmarks of cancer. Cell 2000; 100:57-70.
18. Ikenoue T, Hong S, Inoki K. Monitoring mammalian target of rapamycin (mTOR) activity. Methods Enzymol 2009; 452:165-80.

19. Sinn B, Tallen G, Schroeder G, Grassl B, Schulze J, Budach V, Tinhofer I. Caffeine confers radiosensitization of PTEN-deficient malignant glioma cells by enhancing ionizing radiation-induced G_1 arrest and negatively regulating Akt phosphorylation. Mol Cancer Ther 9:480-8.
20. Sarkaria JN, Busby EC, Tibbetts RS, Roos P, Taya Y, Karnitz LM, Abraham RT. Inhibition of ATM and ATR kinase activities by the radiosensitizing agent, caffeine. Cancer Res 1999; 59:4375-82.
21. Inoki K, Li Y, Xu T, Guan KL. Rheb GTPase is a direct target of TSC2 GAP activity and regulates mTOR signaling. Genes Dev 2003; 17:1829-34.
22. Inoki K, Li Y, Zhu T, Wu J, Guan KL. TSC2 is phosphorylated and inhibited by Akt and suppresses mTOR signalling. Nat Cell Biol 2002; 4:648-57.
23. Garami A, Zwartkruis FJ, Nobukuni T, Joaquin M, Roccio M, Stocker H, et al. Insulin activation of Rheb, a mediator of mTOR/S6K/4E-BP signaling, is inhibited by TSC1 and 2. Mol Cell 2003; 11:1457-66.
24. Muise-Helmericks RC, Grimes HL, Bellacosa A, Malstrom SE, Tsichlis PN, Rosen N. Cyclin D expression is controlled post-transcriptionally via a phosphatidylinositol-3-kinase/Akt-dependent pathway. J Biol Chem 1998; 273:29864-72.
25. Degtyarev M, De Maziere A, Orr C, Lin J, Lee BB, Tien JY, et al. Akt inhibition promotes autophagy and sensitizes PTEN-null tumors to lysosomotropic agents. J Cell Biol 2008; 183:101-16.
26. Wan X, Harkavy B, Shen N, Grohar P, Helman LJ. Rapamycin induces feedback activation of Akt signaling through an IGF-1R-dependent mechanism. Oncogene 2007; 26:1932-40.
27. Sun SY, Rosenberg LM, Wang X, Zhou Z, Yue P, Fu H, Khuri FR. Activation of Akt and eIF4E survival pathways by rapamycin-mediated mammalian target of rapamycin inhibition. Cancer Res 2005; 65:7052-8.
28. O'Reilly KE, Rojo F, She QB, Solit D, Mills GB, Smith D, et al. mTOR inhibition induces upstream receptor tyrosine kinase signaling and activates Akt. Cancer Res 2006; 66:1500-8.
29. Cirstea D, Hideshima T, Rodig S, Santo L, Pozzi S, Vallet S, et al. Dual inhibition of akt/mammalian target of rapamycin pathway by nanoparticle albumin-bound-rapamycin and perifosine induces antitumor activity in multiple myeloma. Mol Cancer Ther 2010; 9:963-75.
30. Aoki H, Takada Y, Kondo S, Sawaya R, Aggarwal BB, Kondo Y. Evidence that curcumin suppresses the growth of malignant gliomas in vitro and in vivo through induction of autophagy: role of Akt and extracellular signal-regulated kinase signaling pathways. Mol Pharmacol 2007; 72:29-39.
31. Ellington AA, Berhow MA, Singletary KW. Inhibition of Akt signaling and enhanced ERK1/2 activity are involved in induction of macroautophagy by triterpenoid B-group soyasaponins in colon cancer cells. Carcinogenesis 2006; 27:298-306.
32. Rubinsztein DC, Gestwicki JE, Murphy LO, Klionsky DJ. Potential therapeutic applications of autophagy. Nat Rev Drug Discov 2007; 6:304-12.
33. Ravikumar B, Vacher C, Berger Z, Davies JE, Luo S, Oroz LG, et al. Inhibition of mTOR induces autophagy and reduces toxicity of polyglutamine expansions in fly and mouse models of Huntington disease. Nat Genet 2004; 36:585-95.
34. Kotake Y, Ohta S. MPP$^+$ analogs acting on mitochondria and inducing neuro-degeneration. Curr Med Chem 2003; 10:2507-16.
35. Hagan MP, Hopcia KL, Sylvester FC, Held KD. Caffeine-induced apoptosis reveals a persistent lesion after treatment with bromodeoxyuridine and ultraviolet-B light. Radiat Res 1997; 147:674-9.
36. Efferth T, Fabry U, Glatte P, Osieka R. Expression of apoptosis-related oncoproteins and modulation of apoptosis by caffeine in human leukemic cells. J Cancer Res Clin Oncol 1995; 121:648-56.
37. Shinomiya N, Takemura T, Iwamoto K, Rokutanda M. Caffeine induces S-phase apoptosis in cis-diamminedichloroplatinum-treated cells, whereas cis-diamminedichloroplatinum induces a block in G_2/M. Cytometry 1997; 27:365-73.
38. Lau CC, Pardee AB. Mechanism by which caffeine potentiates lethality of nitrogen mustard. Proc Natl Acad Sci USA 1982; 79:2942-6.
39. Takagi M, Shigeta T, Asada M, Iwata S, Nakazawa S, Kanke Y, et al. DNA damage-associated cell cycle and cell death control is differentially modulated by caffeine in clones with p53 mutations. Leukemia 1999; 13:70-7.
40. Ormerod MG, Collins MK, Rodriguez-Tarduchy G, Robertson D. Apoptosis in interleukin-3-dependent haemopoietic cells. Quantification by two flow cytometric methods. J Immunol Methods 1992; 153:57-65.
41. Kawatani M, Uchi M, Simizu S, Osada H, Imoto M. Transmembrane domain of Bcl-2 is required for inhibition of ceramide synthesis, but not cytochrome *c* release in the pathway of inostamycin-induced apoptosis. Exp Cell Res 2003; 286:57-66.
42. Kawajiri S, Saiki S, Sato S, Sato F, Hatano T, Eguchi H, Hattori N. PINK1 is recruited to mitochondria with parkin and associates with LC3 in mitophagy. FEBS Lett 2010; 584:1073-9.
43. Sarkar S, Davies JE, Huang Z, Tunnacliffe A, Rubinsztein DC. Trehalose, a novel mTOR-independent autophagy enhancer, accelerates the clearance of mutant huntingtin and alpha-synuclein. J Biol Chem 2007; 282:5641-52.

Journal of Antibiotics (2012) 00, 1–6

www.nature.com/ja

ORIGINAL ARTICLE

Inostamycin enhanced TRAIL-induced apoptosis through DR5 upregulation on the cell surface

Kohta Yamamoto[1], Masafumi Makino[1], Ramida Watanapokasin[2], Etsu Tashiro[1] and Masaya Imoto[1]

Tumor necrosis factor-related apoptosis-inducing ligand (TRAIL) has been considered as a possible therapeutic agent for cancer treatment. This is because of its selective cytotoxicity against various cancer cells without a detrimental effect on normal cells. However, recent studies have reported that the potential application of TRAIL in cancer therapy is limited, as many cancer cells have been found to be resistant to TRAIL. Therefore, small molecule compounds that potentiate the cytotoxicity of TRAIL would be strategic candidates for therapeutic applications in combination with TRAIL. Here we found that a combined treatment of inostamycin and TRAIL synergistically induced caspase-dependent apoptosis in HCT116 cells. Inostamycin upregulated DR5, and a knockdown of DR5 suppressed the apoptosis that was synergistically induced by co-treatment with inostamycin and TRAIL. Moreover, inostamycin increased the expression of DR5 on the cell surface. Therefore, inostamycin-increased cell surface expression of DR5 may have contributed to the enhancement of TRAIL-induced apoptosis. Our study suggests that combined treatment with inostamycin and TRAIL may offer a strategy to overcome TRAIL resistance in tumor cells.
The Journal of Antibiotics advance online publication, 4 April 2012; doi:10.1038/ja.2012.21

Keywords: apoptosis; DR5; inostamycin; TRAIL

INTRODUCTION

Tumor necrosis factor-related apoptosis-inducing ligand (TRAIL), also known as Apo2L, is a type II transmembrane protein. TRAIL was originally identified on the basis of sequence homology to the Fas ligand and tumor necrosis factor.[1,2] TRAIL is hypothesized as being a potentially good therapeutic agent for cancer treatment. This is because TRAIL has been shown to induce apoptosis in a variety of tumor cell lines more efficiently than in normal cells.[3–5] TRAIL exerts its function by binding its receptors, which are expressed on the surface of target cells. To date, four different types of membrane-bound death receptors for TRAIL has been identified: TRAIL-R1/DR4, TRAIL-R2/DR5, TRAIL-R3/DcR1 and TRAIL-R4/DcR2. Both DR4 and DR5 have a conserved cytoplasmic region called the 'death domain'. This is a homolog to Fas and tumor necrosis factor-R1, and is required for TRAIL-induced apoptosis.[6–8] On the other hand, TRAIL also binds to DcR1 and DcR2 that sequester the ligand, but are unable to initiate an apoptosis signal. Thus, DcR1 and DcR2 are considered to be the decoy receptors.[7,9] The apoptosis signal that is induced by TRAIL has been shown to be similar to that which is induced by Fas. The TRAIL homotrimer induces trimerization of DR5 or DR4 on the surface of target cells, which leads to the formation of death-inducing signaling complex. The trimerization of the death domains results in the recruitment of an adaptor molecule Fas-associated protein with death domain (FADD), which in turn recruits and activates caspase-8. In type I cells, activation of caspase- 8 is sufficient for the subsequent activation of effector caspase-3. On the other hand, in type II cells, amplification through the mitochondrial pathway is initiated by the cleavage of Bid by caspase-8. Truncated-Bid causes the loss of mitochondrial membrane potential and caspase-9 cleavage, resulting in the activation of caspase-3 and subsequent cellular apoptosis.

The potential application of TRAIL in cancer therapy is currently limited, as many cancer cells have been found to be resistant to the cytotoxic effects of TRAIL. This resistance may be because of the low expression of pro-apoptotic molecules: death receptors or caspase-8. Alternatively, the resistance may be because of the high expression of anti-apoptotic molecules: decoy receptors, FLICE-like-inhibitory protein, inhibitor of apoptosis protein and Bcl-2. Because of the limitations of TRAIL-induced cytotoxicity, the combination of TRAIL with other small molecule compounds has been postulated as strategy to potentiate the cytotoxicity of TRAIL and its therapeutic applications. Indeed, it was reported that several chemotherapeutic agents and natural products, such as CDDP,[10] etoposide,[10,11] doxorubicin,[12] PS-341 (bortezomib),[13] tunicamycin,[14] rottlerin,[15] brandisianins,[16] silibinin[17] and sodium butyrate,[18] were succeeded to cause the sensitization of TRAIL-resistant tumor cells to TRAIL-induced apoptosis.

In this study, we have screened candidate small molecule compounds that synergistically induce apoptosis in the presence of

[1]Department of Biosciences and Informatics, Faculty of Science and Technology, Keio University, Yokohama, Japan and [2]Department of Biochemistry, Faculty of Medicine, Srinakharinwirot University, Bangkok, Thailand
Correspondence: Dr E Tashiro, Department of Biosciences and Informatics, Faculty of Science and Technology, Keio University, 3-14-1 Hiyoshi, Kohoku-ku, Yokohama, 223-8522, Japan.
E-mail: tashiro@bio.keio.ac.jp
Received 11 January 2012; revised 19 February 2012; accepted 27 February 2012

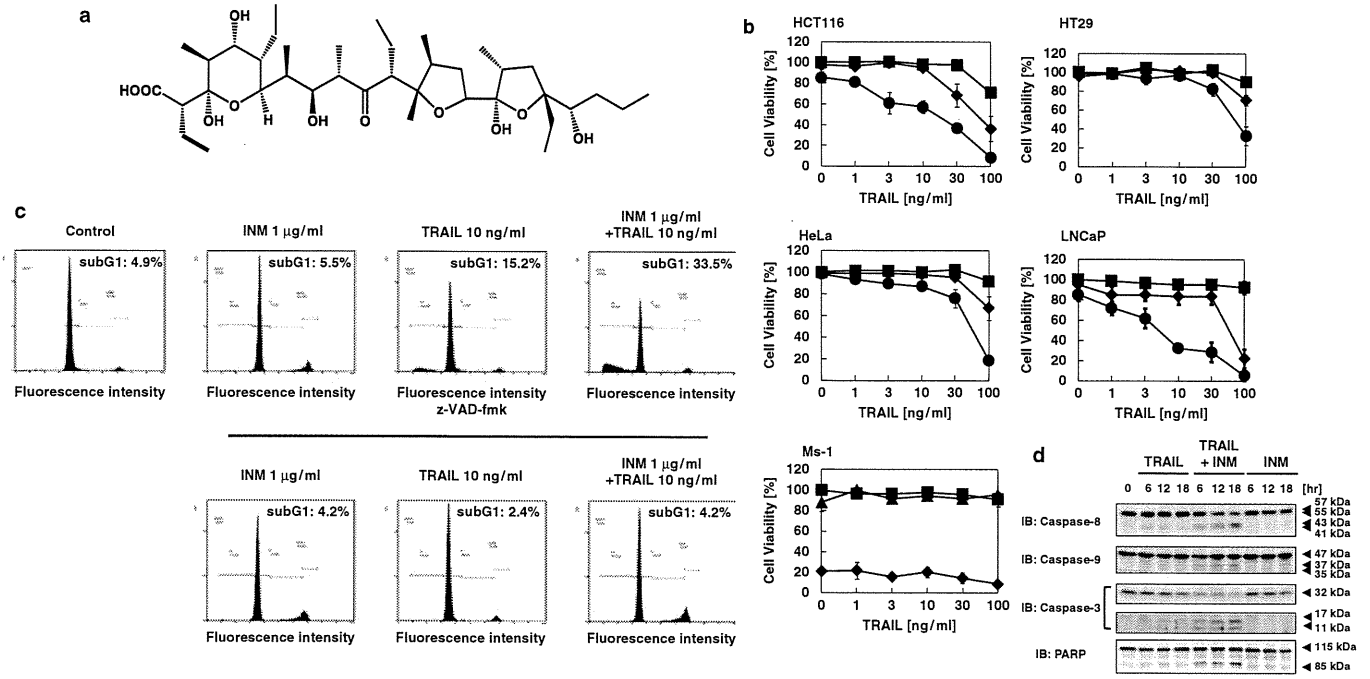

Figure 1 Co-treatment with inostamycin (INM) and tumor necrosis factor-related apoptosis-inducing ligand (TRAIL) synergistically induced apoptosis in HCT116 cells. (**a**) Structure of inostamycin.[19] (**b**) Co-treatment with INM and TRAIL induced a synergistic cytotoxicity in HCT116 cells, HeLa cells, HT29 cells and LNCaP cells, but not in Ms-1 cells. HCT116 cells, HeLa cells, HT29 cells, LNCaP cells or Ms-1 cells were treated with the indicated concentration of TRAIL and 0.0 (square), 0.01 (triangle), 0.1 (diamond-shaped) or 1 (circle) $\mu g\,ml^{-1}$ of INM for 18 h. The cytotoxicity was evaluated using a Trypan Blue Exclusion assay. (**c**) The cytotoxicity induced by the co-treatment with INM and TRAIL was completely suppressed by z-VAD-fmk. HCT116 cells were pre-treated with or without 100 μM of z-VAD-fmk, and then treated further with $10\,ng\,ml^{-1}$ of TRAIL and $1\,\mu g\,ml^{-1}$ of INM. After an 18-h incubation period, the sub-G_1 population was measured by flow cytometer. (**d**) Co-treatment with INM and TRAIL activated caspase. HCT116 cells were treated with or without $10\,ng\,ml^{-1}$ of TRAIL and $1\,\mu g\,ml^{-1}$ of INM for the indicated periods. Cell extracts were prepared for western blotting to detect the expression of caspase-8, caspase-9, caspase-3 and poly(ADP-ribose) polymerase (PARP).

TRAIL. As a result, we found that co-treatment with inostamycin and TRAIL synergistically induced caspase-dependent apoptosis in colorectal cancer HCT116 cells. Inostamycin was isolated from *Streptomyces* species. MH816-AF15;[19] its structure was shown in Figure 1a. Inostamycin weakly upregulated DR4 and strongly upregulated DR5 expression. Additionally, the synergistic apoptosis that was induced by this co-treatment was completely suppressed in DR5 small interfering RNA (siRNA)-transfected but not in DR4 siRNA-transfected HCT116 cells. Furthermore, inostamycin increased cell surface expression of DR5. Taken together with these results, upregulation of cell surface DR5 by inostamycin possibly contributes to the enhancement of TRAIL-induced apoptosis.

MATERIALS AND METHODS

Materials

Inostamycin was prepared as previously described,[19] TRAIL was purchased from Millipore (Billerica, MA, USA). Tunicamycin and z-VAD-fmk were purchased from SIGMA (St. Louis, MO, USA). Rabbit monoclonal anti-poly(ADP-ribose) polymerase, rabbit polyclonal anti-caspase-9, anti-caspase-3, anti-Bcl-xL and mouse monoclonal anti-caspase-8 were purchased from Cell Signaling Technology (Beverly, MA, USA). Rabbit polyclonal anti-survivin was purchased from Santa Cruz Biotechnology (Santa Cruz, CA, USA). Mouse monoclonal anti-X-linked inhibitor of apoptosis protein (XIAP) was purchased from BD Transduction Laboratories (San Diego, CA, USA). Mouse monoclonal anti-Bcl-2 was purchased from Dako (Carpentaria, CA, USA). Rabbit polyclonal anti-DR5 was purchased from Proscience (Poway, CA, USA). Rabbit polyclonal anti-DR4 was purchased from Millipore. Mouse monoclonal anti-C/EBP homologous protein (CHOP) was purchased from Thermo scientific (Rockford, IL, USA). Mouse monoclonal anti-DR5 phycoerythrin (PE)-conjugated was purchased from eBioscience (San Diego, CA, USA). Horseradish peroxidase-conjugated anti-mouse IgG and anti-rabbit IgG secondary antibodies were purchased from GE Healthcare (Little Chalfont, UK).

Cell culture

Human colorectal carcinoma HCT116 cells, HT29 cells and human small cell lung cancer Ms-1 cells were maintained in Roswell Park Memorial Institute medium (Nissui, Tokyo, Japan) supplemented with 5% fetal bovine serum. Human cervical cancer HeLa cells were maintained in Dulbecco's modified Eagle's medium (Nissui, Tokyo, Japan) supplemented with 8% fetal bovine serum. Human prostate adenocarcinoma LNCaP cells were maintained in Roswell Park Memorial Institute medium supplemented with 10% fetal bovine serum— Roswell Park Memorial Institute medium.

Trypan blue exclusion assay

HCT116 cells, HT29 cells, HeLa cells, LNCaP cells or Ms−1 cells were seeded in 48-well plates and incubated overnight, before experiments were conducted. The cells were treated with TRAIL with or without inostamycin for 18 h. Floating and adherent cells were collected and resuspended in phosphate-buffered saline (PBS^-). Cells were mixed with trypan blue and counted under the microscope.

Propidium iodide staining

Propidium iodide staining and flow cytometry were used to determine the degree of cellular apoptosis. HCT116 cells were seeded in 6-well plates and incubated overnight before experiment. The cells were treated with TRAIL with or without inostamycin for 18 h. Floating and adherent cells were collected and resuspended in PBS^-. Cold ethanol was added in a dropwise manner while vortexing to fix the cells. Fixed cells were collected and resuspended in PBS^- containing $50\,\mu g\,ml^{-1}$ propidium iodide. Flow cytometry was done using

EPICS (Beckman Coulter, Fullerton CA, USA). The percentage of sub-G_1 cells was used to quantify apoptotic cells.

Western blotting

Cells were lysed with a lysis buffer containing 25 mM HEPES (pH 7.8), 1.5% Triton-X 100, 1.0% sodium deoxycholate, 0.1% SDS, 0.5 M NaCl, 5 mM EDTA, 50 mM NaF, 100 μM Na_3VO_4, 0.1 mg ml^{-1} leupeptin and 1 mM phenylmethylsulfonyl fluoride. Proteins were separated by SDS—polyacryalamide gel electrophoresis and transferred to a polyvinylidene fluoride membrane (Millipore). After the membranes had been incubated with primary and secondary antibodies, the immune complexes were detected with an Immobilon Western kit (Millipore), and the luminescence was detected with a LAS-1000 mini (Fujifilm, Tokyo, Japan).

Real-time reverse transcriptase (RT)–PCR analysis

Total RNA was isolated with TRIzol (Invitrogen, Carlsbad, CA, USA). Reverse transcription was performed with M-MLV reverse transcriptase (PROMEGA, Madison, WI, USA) according to the manufacturer's instructions. Real-time reverse transcription (RT)–PCR was performed using SYBR Premix Ex Taq (Takara, Shiga, Japan). Primer sequence was as follows: DR5, 5′-CACCA GGTGTGATTCAGGTG-3′ (sense) and 5′-TACGGCTGCAACTGTGACTC-3′ (antisense); CHOP, 5′-GCGCATGAAGGAGAAAGAAC-3′ (sense) and 5′-TCACCATTCGGTCAATCAGA-3′ (antisense); glyceraldehyde-3-phosphate dehydrogenase, 5′-AGGTCGGAGTCAACGGATTT-3′ (sense) and 5′-TAGTTG AGGTCAATGAAGGG-3′ (antisense).

RNA interference

siRNA for control (12935-300), CHOP (5′-CCUCACUCUCCAGAUUCCA GUCAGA-3′) DR4 (HSS112945) and DR5 (HSS112939) were purchased from Invitrogen. HCT116 cells were transfected with siRNA using HiPerFect (QIAGEN, Hilden, Germany), according to the manufacturer's instructions.

Cell surface staining of DR5

HCT116 cells were seeded in 6-well plates and incubated overnight before the experiment. Cells were then treated with inostamycin for 12 h. Cells were then collected and resuspended in PBS$^-$ including PE-conjugated DR5 antibody. After incubation for 1 h at 4 °C, the cells were washed with PBS$^-$ twice and resuspended in PBS$^-$. Flow cytometry analysis was performed with EPICS (Beckman Coulter).

RESULTS AND DISCUSSION

Co-treatment with inostamycin and TRAIL synergistically induced apoptosis in HCT116 cells

In this study, we first found that co-treatment with inostamycin and TRAIL synergistically induced cytotoxicity in HCT116 cells. As shown in Figure 1b, although neither 10 ng ml^{-1} TRAIL nor 1 μg ml^{-1} inostamycin alone showed cytotoxicity in HCT116 cells after 18 h treatment, the cell viability was decreased to about 40% when HCT116 cells were treated with inostamycin and TRAIL in combination. The synergistic cytotoxicity occurred in inostamycin and TRAIL dose-dependent manner. This synergistic effect is cell type-dependent, and is observed in HeLa cells, HT29 cells and LNCaP cells but not in Ms-1 cells (Figure 1b). Flow cytometer analysis demonstrated that the synergistic increase of the Sub-G_1 population was observed in co-treatment with inostamycin and TRAIL in HCT116 cells (Figure 1c). Furthermore, a one hour preincubation with the pan-caspase inhibitor 100 μM z-VAD-fmk suppressed the cell death that was induced by co-treatment with inostamycin and TRAIL (Figure 1c). We also observed the cleavage of caspase-8, caspase-9, caspase-3 and poly(ADP-ribose) polymerase, a well known substrate of caspase-3, at 6 h after inostamycin and TRAIL co-treatment (Figure 1d). In contrast, the cleaved caspase-8, caspase-9, caspase-3 and poly(ADP-ribose) polymerase were only weakly detected when HCT116 cells were treated with 10 ng ml^{-1} of TRAIL alone. Inostamycin alone also could not activate caspase-8, caspase-9 or caspase-3 in HCT116 cells (Figure 1d). These results suggested that co-treatment with inostamycin and TRAIL induced caspase-dependent apoptosis.

Inostamycin enhanced TRAIL-induced apoptosis possibly through DR5 upregulation on the cell surface

TRAIL-stimulated death signal is initiated by the binding of TRAIL to DR4 or DR5, which resulted in the subsequent activation of caspase-8. As shown in Figure 2a, western blotting analysis using an anti-DR4 or anti-DR5 antibody showed that inostamycin strongly upregulated the DR5 protein in HCT116 cells, it also slightly upregulated the DR4 protein (Figure 2a). Similarly, inostamycin-induced DR5 upregulation was also observed in HT29 cells and HeLa cells, in which co-treatment with inostamycin and TRAIL induced synergistic cytotoxicity (Figure 2a). Inostamycin-induced DR5 protein was detected as two bands, which were likely products of alternative splice variants of the DR5 gene[20,21] Furthermore, under the condition where inostamycin-upregulated DR4 or -DR5 protein was efficiently reduced by transient transfection of DR4 siRNA or DR5 siRNA (Figure 2b), apoptosis induced by co-treatment with inostamycin and TRAIL was completely suppressed in DR5 siRNA-transfected HCT116 cells, but not in DR4 siRNA-transfected HCT116 cells (Figure 2c). These results indicated that DR5 is indispensable for the apoptosis induced by co-treatment with inostamycin and TRAIL. Moreover, inostamycin induced cell surface expression of DR5 in a time-dependent manner (Figure 2d). On the other hand, the protein expression of four anti-apoptotic molecules, Bcl-2, Bcl-xL, XIAP and survivin, was unaffected by inostamycin in HCT116 cells (Figure 2e). Considering that it increases the cell surface expression of DR5, it is likely that inostamycin-increased cell surface expression of DR5 contributes to TRAIL sensitization.

Inostamycin-induced transcription of DR5 was regulated by CHOP.

As shown in Figure 3a, inostamycin-induced increases in DR5 mRNA levels were evaluated by real-time RT–PCR analysis. This data suggests that inostamycin activates transcription of DR5 in HCT116 cells. Recent studies have reported that tunicamycin-induced[14] and MG132-induced[22] CHOP (C/EBP homologous protein) upregulation activates DR5 transcription through CHOP-binding site in DR5 promoter region. This results in a sensitization of TRAIL-induced apoptosis. As we also found that 1 μg ml^{-1} inostamycin increased CHOP protein expression with similar time-course kinetics to DR5 upregulation (Figure 3b), we next examined whether this inostamycin-induced CHOP expression regulated DR5 transcription. When CHOP was successfully silenced by transient transfection of siRNA for CHOP (siCHOP) (Figure 3c), inostamycin-increased DR5 mRNA was markedly suppressed (Figure 3d). Furthermore, as consistent with previous report, tunicamycin-increased expression of DR5 mRNA was also completely suppressed in siCHOP-transfected HCT116 cells (Figure 3d). Next, we examined whether inostamycin-induced DR5 protein upregulation was also suppressed in CHOP-knockdown HCT116 cells. As shown in Figures 4a and b, neither inostamycin-induced DR5 protein expression nor inostamycin-increased cell surface expression of DR5 was suppressed under the conditions where tunicamycin-induced DR5 protein expression was completely suppressed in CHOP-knockdown cells. Furthermore, the transient transfection with siCHOP could not suppress apoptosis induction by the synergistic effect of co-treatment with inostamycin and TRAIL (Figure 4c).

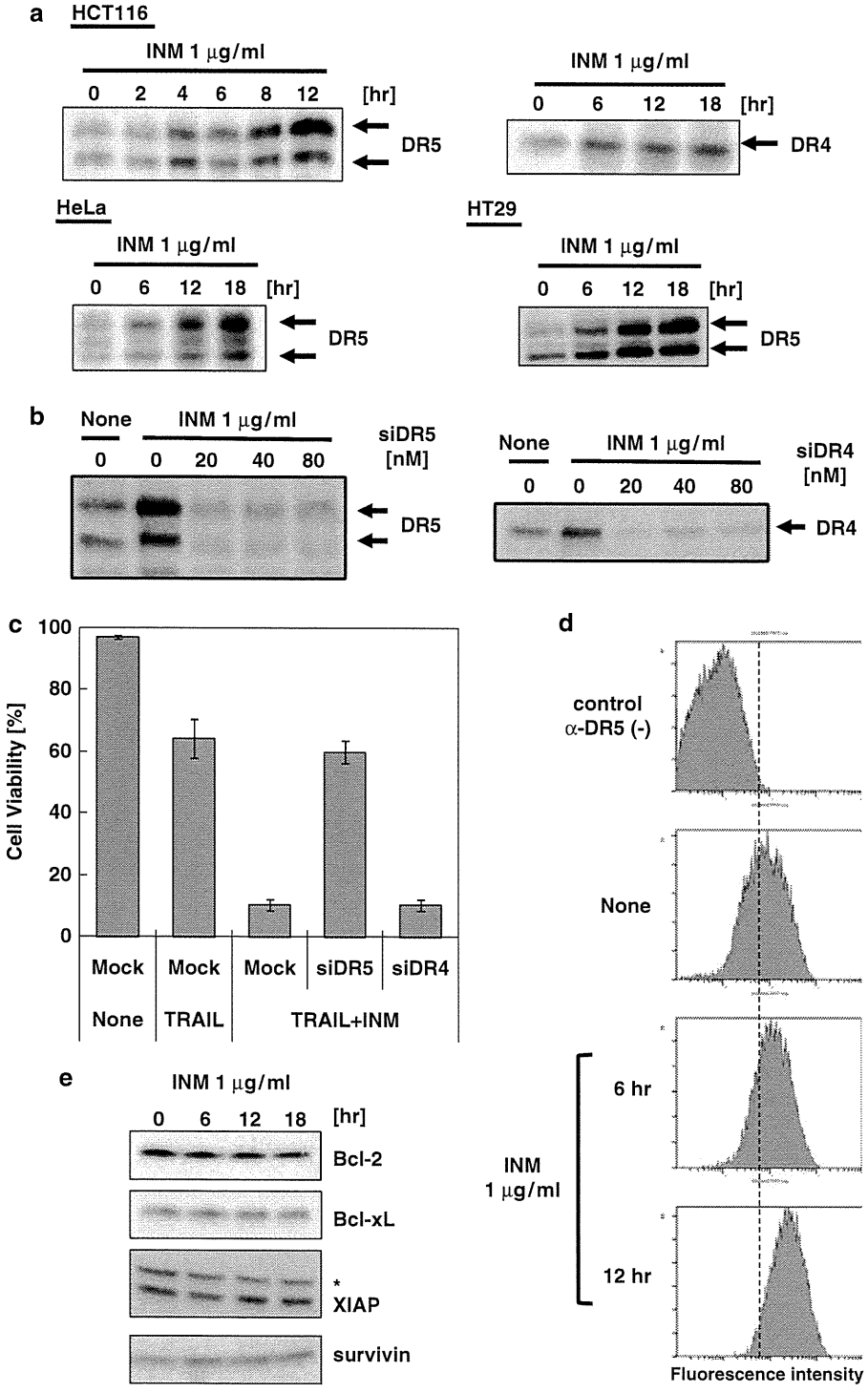

Figure 2 Inostamycin (INM) increased cell surface expression of DR5 in HCT116 cells. (**a**) Effect of INM on the expression of DR4 and DR5 in HCT116 cells, and DR5 in HeLa cells and HT29 cells. HCT116 cells, HeLa cells and HT29 cells were treated with 1 μg ml^{-1} of INM for the indicated periods. Cell extracts were prepared for western blotting to detect the expression of DR4 and DR5. (**b**) Transient transfection of small interfering RNA (siRNA) against DR4 or DR5 suppressed INM-induced DR4 or DR5 expression in HCT116 cells. HCT116 cells were transiently transfected with the indicated concentration of DR4 siRNA (siDR4) or DR5 siRNA (siDR5). After incubation for 24 h, the transfected cells were treated with 1 μg ml^{-1} of INM for 12 h. Cell extracts were prepared for western blotting to detect the expression of DR4 and DR5. (**c**) Knockdown of DR5 suppressed synergistic apoptosis induction by co-treatment with INM and tumor necrosis factor-related apoptosis-inducing ligand (TRAIL). HCT116 cells were transiently transfected with 20 nM DR4 siRNA (siDR4) or siDR5. After incubation for 24 h, the transfected cells were treated with or without 1 μg ml^{-1} INM together with 10 ng ml^{-1} TRAIL for more 24 h. The cell viability was evaluated using a Trypan Blue Exclusion assay. (**d**) INM increased the cell surface expression of DR5 in HCT116 cells. HCT116 cells were treated with 1 μg ml^{-1} of INM for 6 or 12 h. The cell surface DR5 were stained with or without PE-conjugated DR5 antibody and then further detected with flow cytometer. (**e**) INM did not affect the expression of anti-apoptotic proteins in HCT116 cells. HCT116 cells were treated with 1 μg ml^{-1} of INM for the indicated periods. Cell extracts were prepared for western blotting to detect the expression of Bcl-2, Bcl-xL, XIAP and survivin. * indicates non-specific band.

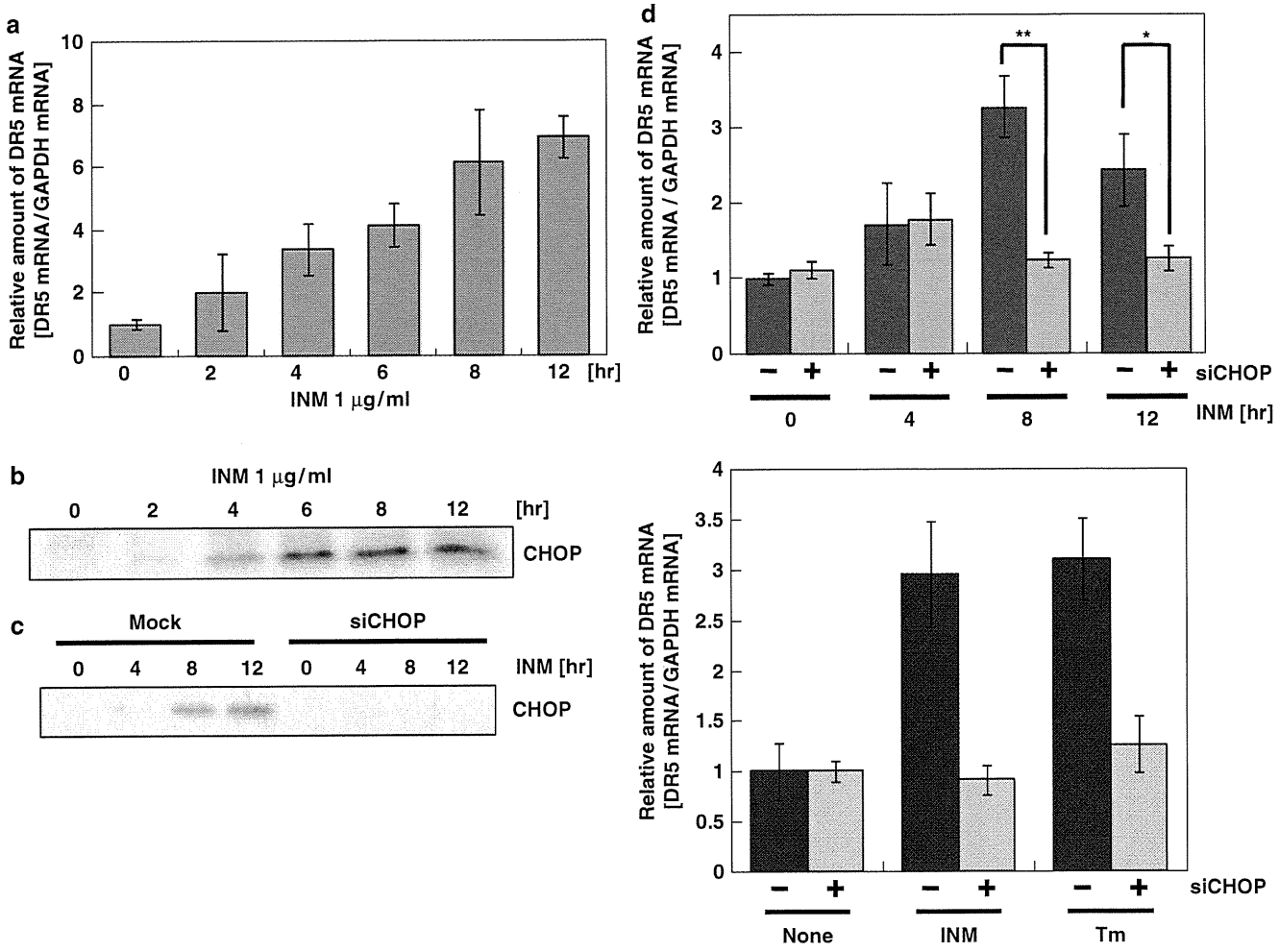

Figure 3 Inostamycin (INM) activated DR5 transcription through CHOP upregulation. (**a**) INM induced DR5 upregulation of mRNA levels in HCT116 cells. HCT116 cells were treated with 1 μg ml^{-1} of INM for the indicated periods. The cells were collected and RNA was extracted. DR5 mRNA levels were evaluated by real-time RT–PCR. DR5 mRNA was normalized with the mRNA levels of glyceraldehyde-3-phosphate dehydrogenase. Data are the means ± s.d. among three independent experiments. (**b**) Effect of INM on the expression of CHOP in HCT116 cells. HCT116 cells were treated with 1 μg ml^{-1} of INM for the indicated periods. Cell extracts were prepared for western blotting to detect the expression of CHOP. (**c**) Transient transfection of small interfering RNA (siRNA) against CHOP suppressed INM-induced CHOP expression in HCT116 cells. HCT116 cells were transiently transfected with 20 nM siCHOP. After 24 h incubation, the transfected cells were treated with 1 μg ml^{-1} of INM for 4, 8 or 12 h. Cell extracts were prepared for western blotting to detect the expression of CHOP. (**d**) Knockdown of CHOP suppressed INM- and tunicamycin (Tm)-induced DR5 upregulation at mRNA levels. HCT116 cells were transiently transfected with 20 nM siCHOP. After incubation for 24 h, the transfected cells were treated with 1 μg ml^{-1} of INM for 4, 8 or 12 h or 10 μg ml^{-1} of Tm for 12 h. The cells were collected and RNA was extracted. DR5 mRNA levels were evaluated by real-time RT–PCR. DR5 mRNA was normalized with the mRNA levels of glyceraldehyde-3-phosphate dehydrogenase (GAPDH). Data are the means ± s.d. among three independent experiments. $^{*}P<0.05$ and $^{**}P<0.005$.

When considered together, our results suggest that inostamycin enhanced TRAIL-induced apoptosis possibly because of a CHOP-independent upregulation of DR5 on the cell surface. At present, the mechanism by which inostamycin upregulates DR5 protein expression remains unclear. However, these results were consistent with our conclusion that the inostamycin-increased cell surface expression of DR5 possibly contributes to the enhancement of TRAIL-induced apoptosis.

In a previous study, various small molecule compounds, such as tunicamycin,[14] were reported to transactivate the DR5 gene by the upregulation of CHOP. The inostamycin-induced increase in DR5 mRNA was suppressed in CHOP-knockdown HCT116 cells; however, DR5 protein expression was not suppressed. Furthermore, knockdown of CHOP by siCHOP suppressed only inostamycin-increased CHOP-dependent DR5 mRNA expression, but constitutively expressed DR5 mRNA levels were not affected (Figure 3d). Therefore, in siCHOP-transfected HCT116 cells, inostamycin is considered to increase the protein levels of DR5 translated from constitutively expressed DR5 mRNA by posttranslational modulation. Various studies have reported the mechanism of the transcriptional activation of DR5 gene. However, little is known about the mechanism of translation, posttranslational modification, localization or degradation of DR5. Because of the data presented in this study, inostamycin may be a good bioprobe for use in investigating the regulatory mechanism of DR5 protein. Furthermore, elucidation of the mechanism by which inostamycin increases the expression of DR5 on the cell surface may provide a new molecular target for inducing DR5 upregulation to overcome TRAIL resistance.

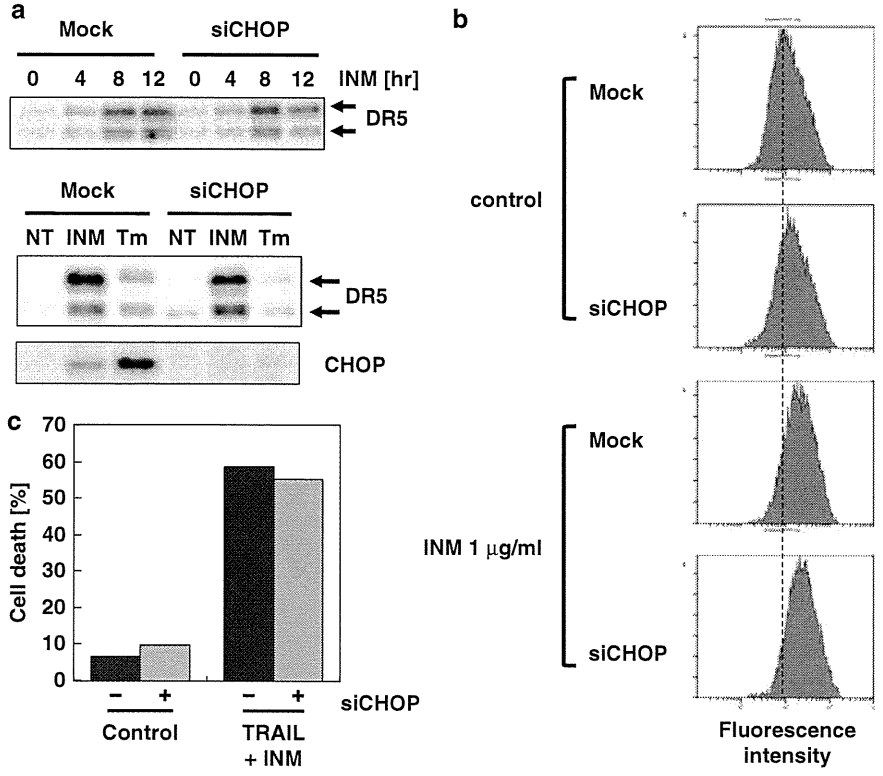

Figure 4 Inostamycin (INM) enhanced tumor necrosis factor-related apoptosis-inducing ligand (TRAIL)-induced apoptosis possibly through CHOP-independent cell surface DR5 upregulation. (**a**) Knockdown of CHOP suppressed tunicamycin (Tm)-induced DR5 upregulation but did not suppress INM-induced DR5 upregulation at protein levels. HCT116 cells were transiently transfected with 20 nM siCHOP. After incubation for 24 h, the transfected cells were treated with 1 $\mu g ml^{-1}$ of INM for 4, 8, 12 h or 10 $\mu g ml^{-1}$ of Tm for 12 h. Cell extracts were prepared for western blotting to detect the expression of DR5. (**b**) Knockdown of CHOP did not suppress the INM-induced upregulation of cell surface DR5. HCT116 cells were transiently transfected with 20 nM siCHOP. After incubation for 24 h, the transfected cells were treated with 1 $\mu g ml^{-1}$ of INM for 12 h. The cell surface DR5 was stained with PE-conjugated DR5 antibody and then detected using a flow cytometer. (**c**) Knockdown of CHOP did not suppress the induction of apoptosis by co-treatment with INM and TRAIL. HCT116 cells were transiently transfected with 20 nM siCHOP. After incubation for 24 h, the transfected cells were treated with or without 1 $\mu g ml^{-1}$ INM together with 10 $ng ml^{-1}$ TRAIL for 18 h. The cells were stained with propidium iodide (PI), and sub-G_1 phase cells were detected using a flow cytometer.

ACKNOWLEDGEMENTS

This work was supported by a Grant-in-Aid for Scientific Research from the Ministry of Education, Culture, Sports, Science and Technology of Japan. This study was partially supported by the Global COE program for Human Metabolomic Systems Biology from MEXT, Japan.

1 Wiley, S. R. *et al.* Identification and characterization of a new member of the TNF family that induces apoptosis. *Immunity* **3,** 673–682 (1995).
2 Pitti, R. M. *et al.* Induction of apoptosis by Apo-2 ligand, a new member of the tumor necrosis factor cytokine family. *J. Biol. Chem.* **271,** 12687–12690 (1996).
3 Ashkenazi, A. & Dixit, V. M. Death receptors: signaling and modulation. *Science* **281,** 1305–1308 (1998).
4 Zhang, X. D. *et al.* Relation of TNF-related apoptosis-inducing ligand (TRAIL) receptor and FLICE-inhibitory protein expression to TRAIL-induced apoptosis of melanoma. *Cancer Res.* **59,** 2747–2753 (1999).
5 Walczak, H. *et al.* Tumoricidal activity of tumor necrosis factor-related apoptosis-inducing ligand *in vivo*. *Nat. Med.* **5,** 157–163 (1999).
6 Pan, G. *et al.* The receptor for the cytotoxic ligand TRAIL. *Science* **276,** 111–113 (1997).
7 Pan, G. *et al.* An antagonist decoy receptor and a death domain-containing receptor for TRAIL. *Science* **277,** 815–818 (1997).
8 Ashkenazi, A. & Dixit, V. M. Apoptosis control by death and decoy receptors. *Curr. Opin. Cell. Biol.* **11,** 255–260 (1999).
9 Sheridan, J. P. *et al.* Control of TRAIL-induced apoptosis by a family of signaling and decoy receptors. *Science* **277,** 818–821 (1997).
10 Nagane, M. *et al.* Increased death receptor 5 expression by chemotherapeutic agents in human gliomas causes synergistic cytotoxicity with tumor necrosis factor-related apoptosis-inducing ligand *in vitro* and *in vivo*. *Cancer Res.* **60,** 847–853 (2000).
11 Wu, G. S. *et al.* KILLER/DR5 is a DNA damage-inducible p53-regulated death receptor gene. *Nat. Genet.* **17,** 141–143 (1997).
12 Sheikh, M. S. *et al.* p53-dependent and -independent regulation of the death receptor KILLER/DR5 gene expression in response to genotoxic stress and tumor necrosis factor alpha. *Cancer Res.* **58,** 1593–1598 (1998).
13 Liu, X. *et al.* The proteasome inhibitor PS-341 (bortezomib) up-regulates DR5 expression leading to induction of apoptosis and enhancement of TRAIL-induced apoptosis despite up-regulation of c-FLIP and survivin expression in human NSCLC cells. *Cancer Res.* **67,** 4981–4988 (2007).
14 Shiraishi, T. *et al.* Tunicamycin enhances tumor necrosis factor-related apoptosis-inducing ligand-induced apoptosis in human prostate cancer cells. *Cancer Res.* **65,** 6364–6370 (2005).
15 Lim, J. H., Park, J. W., Choi, K. S., Park, Y. B. & Kwon, T. K. Rottlerin induces apoptosis via death receptor 5 (DR5) upregulation through CHOP-dependent and PKC delta-independent mechanism in human malignant tumor cells. *Carcinogenesis* **30,** 729–736 (2009).
16 Kikuchi, H. *et al.* Brandisianins A-F, isoflavonoids isolated from Millettia brandisiana in a screening program for death-receptor expression enhancement activity. *J. Nat. Prod.* **70,** 1910–1914 (2007).
17 Son, Y. G. *et al.* Silibinin sensitizes human glioma cells to TRAIL-mediated apoptosis via DR5 up-regulation and down-regulation of c-FLIP and survivin. *Cancer Res.* **67,** 8274–8284 (2007).
18 Kim, Y. H., Park, J. W., Lee, J. Y. & Kwon, T. K. Sodium butyrate sensitizes TRAIL-mediated apoptosis by induction of transcription from the DR5 gene promoter through Sp1 sites in colon cancer cells. *Carcinogenesis* **25,** 1813–1820 (2004).
19 Imoto, M. *et al.* Isolation and structure determination of inostamycin, a novel inhibitor of phosphatidylinositol turnover. *J. Nat. Prod.* **53,** 825–829 (1990).
20 Walczak, H. *et al.* TRAIL-R2: a novel apoptosis-mediating receptor for TRAIL. *Embo. J.* **16,** 5386–5397 (1997).
21 Screaton, G. R. *et al.* TRICK2, a new alternatively spliced receptor that transduces the cytotoxic signal from TRAIL. *Curr. Biol.* **7,** 693–696 (1997).
22 Yoshida, T. *et al.* Proteasome inhibitor MG132 induces death receptor 5 through CCAAT/enhancer-binding protein homologous protein. *Cancer Res.* **65,** 5662–5667 (2005).

ACS chemical biology

Articles

pubs.acs.org/acschemicalbiology

Xanthohumol Impairs Autophagosome Maturation through Direct Inhibition of Valosin-Containing Protein

Yukiko Sasazawa,[†,#] Shuhei Kanagaki,[†,#] Etsu Tashiro,[†] Toshihiko Nogawa,[‡] Makoto Muroi,[‡] Yasumitsu Kondoh,[‡] Hiroyuki Osada,[‡] and Masaya Imoto*[,†]

[†]Faculty of Science and Technology, Department of Biosciences and Informatics, Keio University, Yokohama 223-8522, Japan

[‡]Chemical Biology Core Facility, Chemical Biology Department, RIKEN Advanced Science Institute, Saitama 351-0198, Japan

ABSTRACT: Autophagy is a bulk, nonspecific protein degradation pathway that is involved in the pathogenesis of cancer and neurodegenerative disease. Here, we observed that xanthohumol (XN), a prenylated chalcone present in hops (*Humulus lupulus* L.) and beer, modulates autophagy. By using XN-immobilized beads, valosin-containing protein (VCP) was identified as a XN-binding protein. VCP has been reported to be an essential protein for autophagosome maturation. Using an *in vitro* pull down assay, we showed that XN bound directly to the N domain, which is known to mediate cofactor and substrate binding to VCP. These data indicated that XN inhibited the function of VCP, thereby allowing the impairment of autophagosome maturation and resulting in the accumulation of microtubule-associated protein 1 light chain 3-II (LC3-II). This is the first report demonstrating XN as a VCP inhibitor that binds directly to the N domain of VCP. Our finding that XN bound to and inactivated VCP not only reveals the molecular mechanism of XN-modulated autophagy but may also explain how XN exhibits various biological activities that have been reported previously.

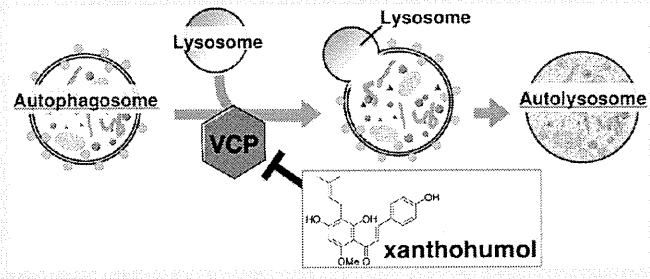

Macroautophagy (herein referred to as autophagy) is an evolutionarily conserved pathway for degradation of intracellular components including organelles, which is critical for the maintenance of cellular homeostasis. Initially, the cytoplasmic components are sequestered by a unique membrane, referred to as an isolation membrane. Dynamic membrane organization is activated from small membrane particles to autophagosomes by the recruitment of autophagy related genes (ATGs) and microtubule-associated 1 light chain 3 (LC3).[1]

The next stage involves the fusion of autophagosomes with lysosomes and subsequent formation of autolysosomes. The inner membrane of the autophagosomes and the cytoplasm-derived materials contained in the autophagosomes are then degraded by lysosomal hydrolases.[2] The amino acids, which are produced by protein degradation, are then returned to the cytoplasm by lysosomal membrane permeases for reuse. Autophagy occurs in all cells at low basal levels under normal conditions to maintain homeostasis. It has been reported that aberrance of autophagy is involved in the pathogenesis of many diseases including neurodegenerative disease,[3,4] cancer,[5] muscle atrophy, and type 2 diabetes.[6]

Despite identification of more than 30 ATGs,[7,8] the molecular mechanism of autophagy is still not fully understood. Studying autophagy through chemical genetics could be an ideal approach to gaining a better understanding of autophagy signaling pathways. Most compounds that have been reported to be regulators of autophagy are distributed between two major groups. One group induces autophagy by inhibiting PI3K/Akt/mTOR signaling,[9] which is the major inhibitory signal that suppresses autophagy. The other group of regulators suppresses autophagy by inhibiting class III PI3K,[10] which is the homologue of yeast VPS34 and is required for the onset of autophagy.

In this study, we explored the mechanism of autophagy and identified additional small compounds that could modulate this process. This was done by screening for a small compound from an in-house natural product library using EGFP-LC3 stably expressing HeLa cells, and we identified xanthohumol (XN) as an autophagy modulator. Xanthohumol (30-[3,3-dimethyl allyl]-20,40,4-trihydroxy-60-methoxychalcone) is the principal prenylated chalcone of the female inflorescences of the hop plant ("hops"), an ingredient of beer.[11] Human exposure to XN is primarily through beer consumption. Several studies have reported on the potential health benefits of XN, including inhibition of diacylglycerol acyltransferase,[12,13] apoptosis induction,[14] NF-kappa B inhibition,[15] and ER stress induction.[16] However, there are no reports that show the relevance of XN to autophagy. Thus, to understand the mechanism by which XN modulates autophagy, we attempted to identify the target protein of XN responsible for the regulation of autophagy.

Received: November 28, 2011
Accepted: February 23, 2012

   dx.doi.org/10.1021/cb200492h | *ACS Chem. Biol.* XXXX, XXX, XXX–XXX

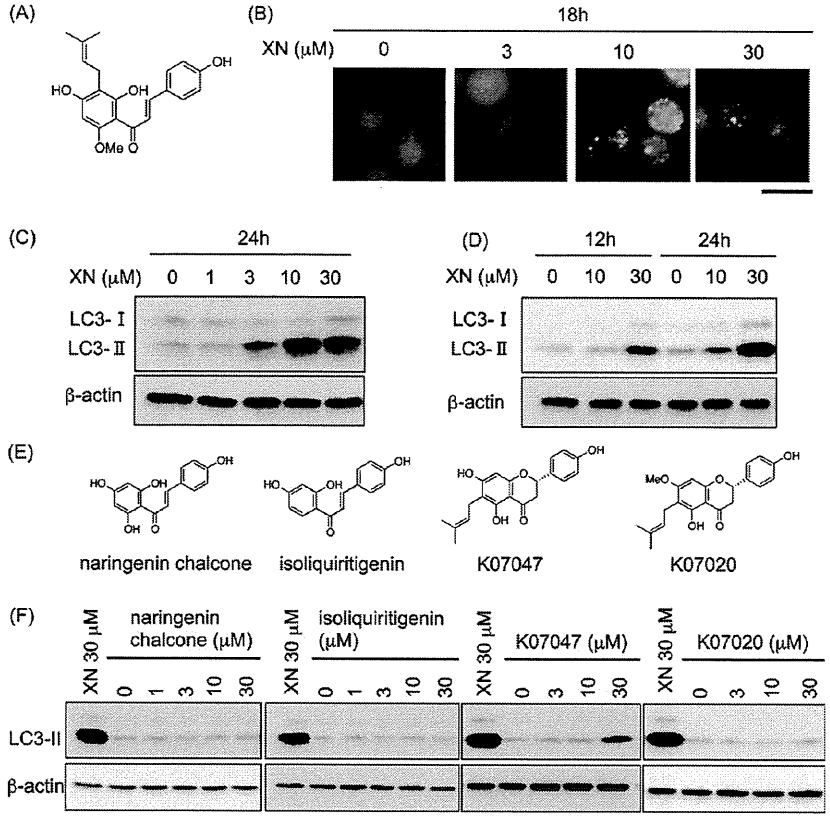

Figure 1. XN modulated autophagy. (A) Structure of xanthohumol (XN). (B) GFP-microtubule-associated protein 1 light chain 3 (LC3) stably expressing HeLa cells were treated with various concentrations of XN for 18 h. Cells were fixed with 3% (w/v) paraformaldehyde and observed under a fluorescence microscope (scale bar, 20 μm). (C) HeLa cells were treated with various concentrations of XN for 24 h. Cell lysates were immunoblotted with anti-LC3B antibody. β-Actin was immunoblotted as a loading control. (D) A431 cells were treated with various concentrations of XN for the indicated time. Cell lysates were immunoblotted with anti-LC3B antibody. β-Actin was immunoblotted as a loading control. (E) Structures of naringenin chalcone, isoliquiritigenin, K07047, and K07020. (F) A431 cells were treated with various concentrations of naringenin chalcone, isoliquiritigenin, K07047, or K07020 for 24 h. Cell lysates were immunoblotted with anti-LC3B antibody. β-Actin was immunoblotted as a loading control.

RESULTS AND DISCUSSION

Xanthohumol Inhibited Autophagosome Maturation.

In order to identify small compounds that could modulate autophagy and to explore the mechanism of autophagy through chemical genetics, we screened for a small compound from an in-house natural product library. As LC3-II is incorporated into the inner and outer surfaces of autophagosomes, the expression of a green fluorescence protein (GFP)-LC3 fusion protein can be used to identify GFP puncta representing autophagosomes.[17] Using this system to identify compounds that modulate autophagy, we searched for compounds that could increase the number of GFP-LC3 puncta in GFP-LC3 stably expressing human cervical carcinoma HeLa cells and found that xanthohumol (XN) showed this activity (Figure 1A). In untreated cells, GFP-LC3 was observed predominantly as diffuse green fluorescence in the cytoplasm. However, in XN-treated cells, characteristic punctate fluorescent patterns were observed, indicating that XN modulates autophagy in a dose-dependent manner, as shown in Figure 1B. Modulation of autophagy by XN was further confirmed by the detection of LC3-II, which is a phosphatidylethanolamine (PE) conjugated form of LC3, as a faster-migrating band when separated by SDS-PAGE and immunoblotted. As shown in Figure 1C, treatment of HeLa cells with XN for 24 h induced an increase in LC3-II levels in a dose-dependent manner. Similarly, XN increased LC3-II expression levels at 30 μM over 12−24 h in human epidermoid carcinoma A431 cells (Figure 1D). Next, we examined the effect of two other chalcones (naringenin chalcone and isoliquiritigenin) and two natural flavanones (K07047 and K07020) on LC3-II expression level. As a result, K07047 increased LC3-II levels weakly compared to XN, whereas naringenin chalcone, isoliquiritigenin, and K07020 did not increase LC3-II levels (Figure 1E,F)

The increase in LC3-II expression can be associated with either PE conjugation due to enhanced formation of autophagosomes or a block of LC3-II degradation due to impaired maturation of autophagosomes. To distinguish between these two possibilities, we detected expression levels of p62, a protein that is degraded by autophagy and accumulated when autophagy is impaired. Bafilomycin A1 (BMA) is known to prevent autophagosome maturation by inhibiting autophagosome-lysosome fusion[18] and caused an increase in the expression levels of p62 by inhibiting proteolytic degradation in autolysosomes, as shown in Figure 2A. Treatment with 30 μM XN for 24 h increased the expression levels of p62 as well. These data suggested that the increased LC3-II expression mediated by XN was a consequence of a block of autophagosome maturation. To further confirm that XN inhibited autophagosome maturation, we detected the localization of LC3 and lysosome in the presence of pepstatin A plus E64D, which are the lysosomal protease inhibitors, to inhibit the degradation of LC3 after fusion of autophagosome

dx.doi.org/10.1021/cb200492h | ACS Chem. Biol. XXXX, XXX, XXX−XXX

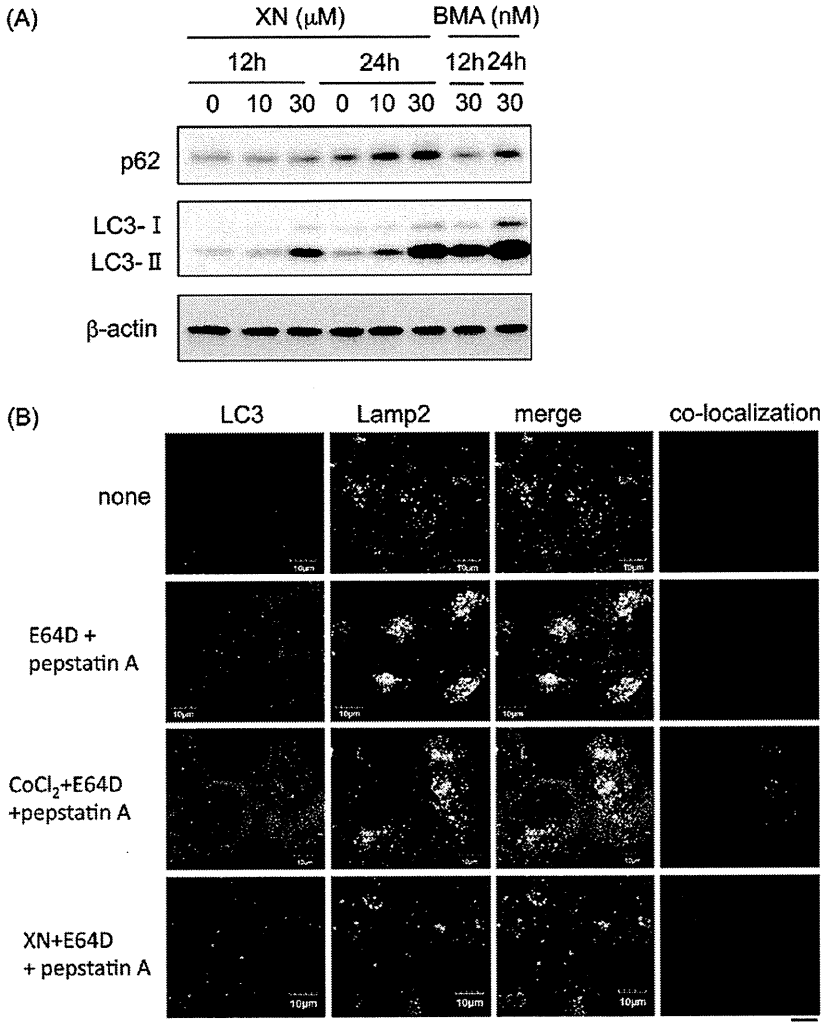

Figure 2. XN inhibited autophagosome maturation. (A) A431 cells were treated with various concentrations of XN or 30 nM bafilomycin A1 (BMA) for the indicated time. Cell lysates were immunoblotted with anti-p62 antibody. β-Actin was immunoblotted as a loading control. (B) A431 cells were treated with 30 μM XN or 0.3 mM $CoCl_2$ in the presence of 30 μM E64D and 30 μM pepstatin A for 24 h. Cells were then fixed with 3% (w/v) paraformaldehyde and immunostained with anti-LC3B and anti-lamp2 antibodies. The cells were observed under confocal microscopy (scale bar, 10 μm).

with lysosome. Because $CoCl_2$ are known to induce an increase in LC3-II expression levels by accelerating autophagosome formation,[19] we examined the effect of XN on the localization of LC3 and lysosome compared with the effect of $CoCl_2$. As shown in Figure 2B, $CoCl_2$ increased the number of LC3-positive puncta co-localizing with lysosome, whereas LC3-positive puncta increased by XN failed to co-localize with lysosome even in the presence of pepstatin A plus E64D. These data strongly indicated that XN impaired autophagosome maturation, resulting in increase in the level of LC3-II.

Identification of XN-Binding Proteins. To elucidate the underlying mechanism behind the suppression of autophagosome maturation induced by XN, we attempted to identify the cellular target protein of XN responsible for autophagy modulation. To this end, we used XN-immobilized agarose beads, which were prepared by a photocross-linking method.[20] A431 cell lysates were incubated for 3 h with XN-immobilized beads (XN beads) or control beads as a negative control. The reacted beads were washed, and the co-precipitated proteins were eluted, separated by SDS-PAGE, and stained with Coomassie brilliant blue (CBB). As shown in Figure 3A, four protein bands that specifically co-precipitated with XN beads were observed. Each protein band was identified by using MALDI-TOF-MS and LC–MS/MS as (i) valosin-containing protein (VCP), (ii) voltage-dependent anion channel (VDAC), (iii) prohibitin-2, and (iv) prohibitin.

Among these proteins, competition was observed only for VCP with 0.1–1 μmol XN as shown in Figure 3B. VCP has been reported to play a role in the maturation of autophagosomes.[21,22] VCP, also known as p97, is one of the best-characterized type II AAA (ATPases associated with diverse cellular activities) ATPases. VCP plays critical roles in a broad range of diverse cellular processes, including ER associated degradation *via* the ubiquitin-proteasome system,[23,24] cell cycle regulation,[25] and DNA repair.[26] Recently, it was reported that VCP is essential for autophagosome–lysosome fusion and formation of autolysosomes in human cell lines.[21,22] Therefore, we speculated that VCP might be the target of XN, and the binding of XN to VCP was confirmed by immunoblotting of co-precipitated protein from XN-beads using anti-VCP antibody (Figure 3C).

XN Bound Directly to the N Domain of VCP. Next, to determine whether XN could bind directly to VCP, we performed an *in vitro* binding assay using purified recombinant

dx.doi.org/10.1021/cb200492h | *ACS Chem. Biol.* XXXX, XXX, XXX–XXX

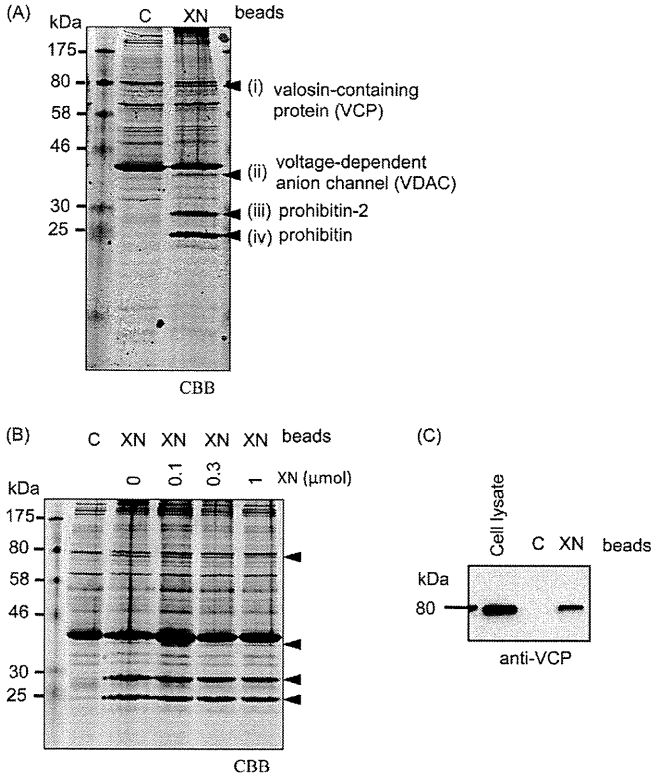

Figure 3. Identification of XN-binding proteins. (A) A431 cell lysates were incubated with control beads or XN beads for 3 h. The reacted beads were washed, and the eluted proteins were subjected to SDS-PAGE and stained by Coomassie brilliant blue (CBB). The co-precipitated proteins for XN beads were identified by using MALDI-TOF-MS and LC–MS/MS. (B) A431 cell lysates were preincubated with 0.1–1 μmol of XN as a competitor for 1 h and then incubated with control beads or XN beads for 3 h. The reacted beads were washed, and the eluted proteins were subjected to SDS-PAGE and stained by CBB. (C) A431 cell lysates were incubated with control beads or XN beads for 3 h. The reacted beads were washed, and the eluted proteins were immunoblotted with anti-valosin-containing protein (VCP) antibody.

GST-tagged VCP protein. Unlike GST, GST-VCP was co-precipitated only with XN-beads, as shown in Figure 4A. Moreover, competition was observed for VCP in the presence of 0.5 μmol of XN (Figure 4B), indicating that XN binds directly to VCP. On the other hand, competition was not observed for binding of XN-beads and VCP in the presence of XN analogues such as naringenin chalcone, isoliquiritigenin, K07047, and K07020 up to 0.5 μmol (Figure 4C), indicating that these analogues bind to VCP very weakly or fail to bind to VCP at least through the XN binding site. Because these analogues fail to induce LC3-II expression level or induce it very weakly, these observations further confirm the importance of the XN binding to VCP for impairment of autophagosome maturation. In addition, because naringenin chalcone and isoliquiritigenin did not bind to VCP, the prenyl and/or *O*-methyl group of XN is thought to be important for binding to VCP.

VCP is composed of a substrate and cofactor binding N domain followed by two AAA ATPase domains, termed D1 and D2, and forms a hexameric double-ring structure.[27,28] It has been demonstrated that both D1 and D2 domain contain Walker A and Walker B motifs that mediate ATP binding and hydrolysis, respectively. However, these two ATPase domains are not catalytically equivalent: D2 domain has the major ATPase activity at physiological temperatures, whereas D1 is involved in the regulation of heat-induced ATPase activity.[29] D1 also plays a major role in hexamerization.[30,31] To determine which domain in VCP is essential for interaction with XN, we prepared three GST-tagged VCP mutants that lacked the N-terminal domain (1–185) (GST-VCPΔN), D1 domain containing Walker A and Walker B motifs (186–348) (GST-VCPΔD1), and D2 domain containing Walker A and Walker B motifs (349–806) (GST-VCPΔD2) (Figure 4D). GST-VCPΔD1 and GST-VCPΔD2 were co-precipitated with XN beads, whereas GST-VCPΔ*N* was not, as shown in Figure 4E. These results indicated that XN bound to the N domain of VCP.

XN Inhibited VCP Function. Next, we examined whether this binding of XN to the N domain of VCP could inhibit VCP function. The structural alteration of the N domain of VCP has been reported to induce impaired maturation of autophagosome as well as impaired ER associated degradation (ERAD),[32] and loss of VCP-mediated ERAD activity leads to accumulation of unfolded protein in the ER, resulting in induction of ER stress.[33] Therefore, we examined the effect of XN on the expression of the ER stress markers CHOP and GRP78. As shown in Figure 5A, treatment with 30 μM XN for 12–24 h increased the protein levels of CHOP and GRP78 significantly in A431 cells, suggesting that XN inhibited VCP-mediated ERAD. On the other hand, Hirabayashi *et al.* reported that inhibition of VCP function by using dominant negative VCP induced cytoplasmic vacuolation.[34] These vacuoles are reported to be a result of abnormal budding and enlargement of the ER.[35] We also observed the presence of microscopic vacuoles not only in VCP knockdown A431 cells by using siRNA (Figure 5B) but also in XN-treated A431 cells (Figure 5C). The successful knockdown of VCP using siRNA and resultant up-regulation of LC3-II was confirmed by immunoblotting, as shown in Figure 5B right. Moreover, the XN analogue K07047, which modulated autophagy weakly, also induced vacuolization weakly compared with XN. On the other hand, other analogues including naringenin chalcone, isoliquiritigenin, and K07020, which had no effect on modulation of autophagy, did not induce vacuolization (Figures 1F and 5C). Taken together, these data indicated that XN bound to the N domain of VCP directly, thereby suppressing VCP function.

Apart from autophagy, XN has been reported to inhibit mitogen/antigen-induced T cell proliferation, development of cell-mediated cytotoxicity, and production of Th1 cytokines by inhibiting NF-κB.[36] Moreover, XN has been shown to inhibit the growth of a wide variety of human cancer cell lines by inhibiting proliferation and inducing apoptosis.[37,38] These previous observations regarding XN suggested the following two possibilities: one possible explanation is that various proteins were interfered with by XN and various biological phenomena were affected, and the other is that XN modulated a specific protein, which was involved in the various biological processes. Our finding that XN modulated the function of VCP may explain how XN exhibited the above-mentioned effects, because VCP is reported to play important roles in the degradation of IκB, resulting in enhancement of NF-κB signaling,[39,40] or because the expression level of VCP is correlated with progression, prognosis, and recurrence of certain types of cancer.[41,42]

Two types of VCP inhibitors have been reported in the literature. The first type of inhibitor is classified as a VCP

dx.doi.org/10.1021/cb200492h | *ACS Chem. Biol.* XXXX, XXX, XXX–XXX

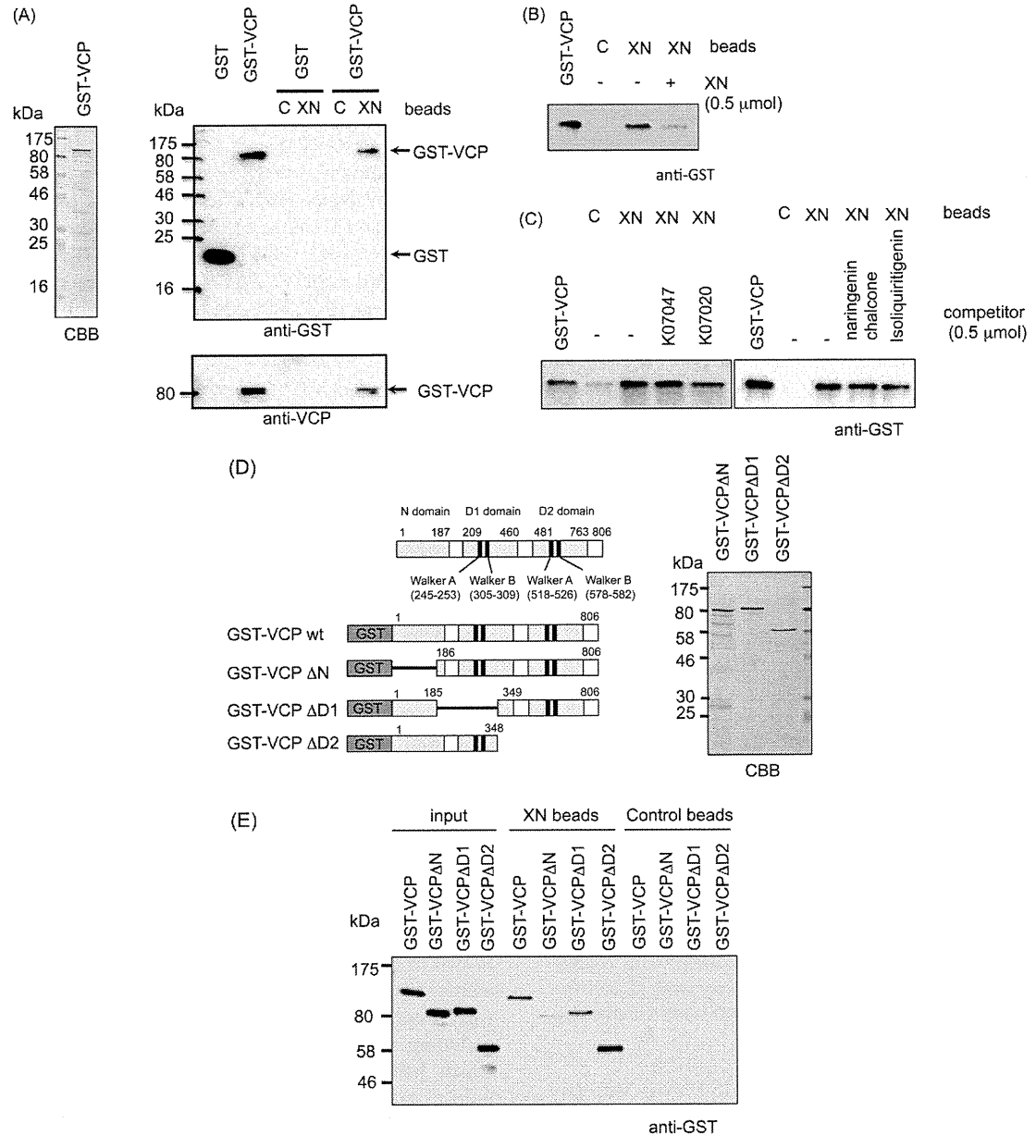

Figure 4. XN bound directly to the N domain of VCP. (A) (left) CBB staining of purified GST-VCP protein. (right) Purified GST and GST-tagged VCP were incubated with control beads or XN beads for 3 h. The reacted beads were washed, and the eluted proteins were immunoblotted with anti-GST and anti-VCP antibodies. (B) Purified GST-tagged VCP was preincubated with 0.5 μmol of XN as a competitor for 1 h and then incubated with control beads or XN beads for 3 h. The reacted beads were washed, and the eluted proteins were immunoblotted with anti-GST antibody. (C) Purified GST-tagged VCP was preincubated with 0.5 μmol of naringenin chalcone, isoliquiritigenin, K07047, or K07020 as a competitor for 1 h and then incubated with control beads or XN beads for 3 h. The reacted beads were washed, and the eluted proteins were immunoblotted with anti-GST antibody. (D) (left) Schematic illustration of GST-VCP, GST-VCPΔN, GST-VCPΔD1, and GST-VCPΔD2. (right) CBB staining of purified GST-VCPΔN, GST-VCPΔD1, and GST-VCPΔD2. (E) Purified GST-VCPΔN, GST-VCPΔD1, and GST-VCPΔD2 were incubated with control beads or XN beads for 3 h. The reacted beads were washed, and the eluted proteins were immunoblotted with anti-GST antibody.

ATPase inhibitor, which most likely binds to a site in the D2 ATPase domain. 2-Anilino-4-aryl-1,3-thiazoles were discovered by high-throughput screening (HTS) as inhibitors of VCP ATPase activity, and these were reported to inhibit VCP-associated protein degradation.[43] Syk inhibitor III was reported to be an irreversible inhibitor of VCP ATPase activity by interacting with CysS22 within the D2 ATPase domain of VCP and the ubiquitin-fused reporter protein.[44] N^2,N^4-Dibenzylquinazoline-2,4-diamine (DBeQ) was identified as a selective, potent, reversible, and ATP-competitive VCP inhibitor by screening a library of chemical compounds.[45] DBeQ blocks multiple processes that have been shown by siRNA to depend on VCP, including degradation of ubiquitin fusion degradation and ERAD as well as autophagosomal maturation. The second type of VCP inhibitor is Eeyarestatin I (Eer I), which binds to the D1 domain of VCP without affecting ATPase activity.[46] Eer I was found to directly associate with the ER membrane and VCP and inhibited VCP-associated deubiquitinating enzymes, thereby inhibiting VCP-dependent protein degradation. However, so far, VCP inhibitors that bind to the N domain of VCP have not yet been reported. Therefore, XN is the first example of such an inhibitor that binds to the N domain of VCP and

dx.doi.org/10.1021/cb200492h | ACS Chem. Biol. XXXX, XXX, XXX–XXX

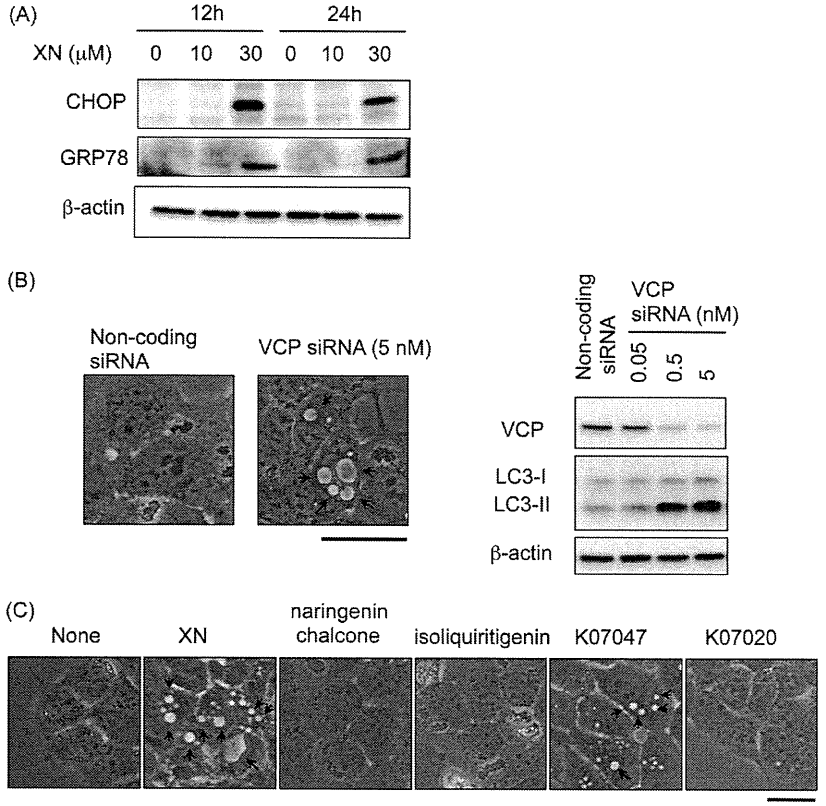

Figure 5. XN inhibited VCP function. (A) A431 cells were treated with various concentrations of XN for the indicated time. Cell lysates were immunoblotted with anti-CHOP and anti-GRP78 antibodies. β-Actin was immunoblotted as a loading control. (B) (left) A431 cells were observed under a microscope 72 h after transfection with non-coding siRNA or VCP siRNA (arrows, vacuoles; scale bar, 25 μm). (right) A431 cells were transfected with VCP siRNA or noncoding siRNA for 72 h. Cell lysates were immunoblotted with anti-VCP and anti-LC3B antibodies. β-Actin was immunoblotted as a loading control. (C) A431 cells were treated with 30 μM XN, naringenin chalcone, isoliquiritigenin, K07047, or K07020 for 24 h and then observed under microscope (arrows, vacuoles; scale bar, 25 μm).

inactivates VCP. Thus, XN is proposed to be a new class of VCP inhibitors, which may be used as a powerful tool for identifying the cofactor or substrate protein of VCP responsible for autophagy regulation.

METHODS

Reagents. Naringenin chalcone was obtained as a generous gift from Kikkoman Corporation. Isoliquiritigenin, E64D, and peptatin A were purchased from Sigma-Aldrich Co.

Cell Line. Human epidermoid carcinoma A431 cells were grown in Dulbecco's modified Eagle medium supplemented with 5% (v/v) calf serum, 100 U mL^{-1} of penicillin G (Sigma-Aldrich Co.), and 0.1 mg mL^{-1} of kanamycin (Sigma-Aldrich Co.) at 37 °C in a 5% CO_2–95% air atmosphere. Human cervical carcinoma HeLa cells were grown in Dulbecco's modified Eagle's medium supplemented with 8% fetal bovine serum, 100 U mL^{-1} of penicillin G, and 0.1 mg mL^{-1} of kanamycin at 37 °C in a 5% CO_2–95% air atmosphere. HeLa/GFP-LC3 stable cell lines were established as previously described.[47]

Isolation of XN from Hop and XN Analogues from Microbial Origin. XN was isolated from commercially available hop extract obtained from Hopsteiner. The extract (200 mg) was purified by using preparative octadecylsilyl (ODS) HPLC (UG 80, 20 mm, 250 mm; SHISEIDO) with 70% (v/v) aqueous MeOH to obtain pure XN (147 mg). The structures were identified by spectroscopic data (NMR and MS). UV (MeOH) λ_{max} (log ε) 369 (4.56); ESIMS m/z 355 $[M + H]^+$; ^{13}C NMR δ192.8, 165.5, 161.8, 161.2, 157.4, 142.0, 136.0, 130.3 (2C), 128.6, 125.5, 121.7, 116.2 (2C), 106.3, 106.2, 105.0, 56.1, 25.8, 21.6, and 17.9. K07020 and K07047 were isolated from 14 L of culture broths of *Streptomyces* sp. HK-803 and *Streptomyces spiroverticillatus* JC-8444 by UV absorption and mass spectra guided separation to afford 10.6 and 9.3 mg as a pale-yellow powder, respectively. The structures were identified by spectroscopic data (NMR and MS). K07020: UV (MeOH) λ_{max} (log ε) 226 (4.45), 288 nm (4.33); ESIMS m/z 353 $[M - H]^-$; ^{13}C NMR δ192.9, 164.6, 163.8, 161.8, 158.8, 131.6, 131.5, 128.9 (2C), 123.9, 116.2 (2C), 110.0, 105.7, 93.5, 80.0, 55.9, 46.2, 26.0, 22.7, and 17.9. K07047: UV (MeOH) λ_{max} (log ε) 226 (4.36), 293 nm (4.24); ESIMS m/z 339 $[M - H]^-$; ^{13}C NMR δ197.8, 165.9, 162.6, 162.5, 159.0, 131.5, 131.2, 129.0 (2C), 123.9, 116.3 (2C), 109.6, 103.2, 95.4, 80.4, 44.2, 25.9, 21.8, and 17.8.

DNA Constructs. Human cDNA for VCP were amplified from A431 cell cDNA and subcloned into pGEX-2T (GE Healthcare UK Ltd.) to prepare GST fusion proteins in bacteria. Expression vectors encoding GST-fused VCP mutants (ΔN, 1–185 aa deletion; ΔD_1, 186–348 aa deletion; and ΔD_2, 349–806 aa deletion) were generated by PCR using pGEX-2T/VCP as a template.

Fluorescence Microscopy. For fluorescence microscopy, HeLa cells stably expressing GFP-LC3, which were grown on coverslips, were treated with chemicals for the indicated time at 37 °C. Cells were fixed with 3% (w/v) paraformaldehyde in PBS at RT. The cells were then washed with PBS and observed under a fluorescence microscope (Olympus).

Western blotting. Cells were lysed with RIPA buffer [25 mM HEPES, 1.5% (v/v) TX-100, 1% (w/v) sodium deoxycholate, 0.1% (w/v) SDS, 0.5 M NaCl, 5 mM EDTA, 50 mM NaF, 100 mM Na_3VO_4, 0.1 mg mL^{-1} leupeptin, 1 mM PMSF; pH 7.8]. Proteins were separated by SDS-PAGE, transferred to a PVDF membrane (Millipore), and probed with specific antibodies. This was followed by detection using the ECL Western blotting detection system (Millipore) and LAS-1000 (Fuji Film). The primary antibodies used were as follows: anti-LC3B (L7543, Sigma-Aldrich Co.), anti-β-actin (AC-74, Sigma-Aldrich Co.), anti-p62 (5114, Cell Signaling Technology), anti-VCP (ab 11433, Abcam), anti-GST (B-14, Santa

dx.doi.org/10.1021/cb200492h | ACS Chem. Biol. XXXX, XXX, XXX–XXX

Cruz Biotechnology), anti-GRP78 (H-129, Santa Cruz Biotechnology), and anti-CHOP (MA1-250, Thermo Fisher Scientific Inc.) antibodies. The secondary antibodies were horseradish peroxidase-conjugated anti-mouse IgG and anti-rabbit IgG (GE Healthcare UK Ltd.).

Immunofluorescent Microscopy. Immunofluorescent microscopy was carried out as previously described.[48] Fluorescence images were obtained using a confocal laser scanning microscope system FV1000 (Olympus).

Detection of Binding Proteins for XN Beads. XN beads were prepared as previously described.[20] A431 cells were harvested, washed with PBS, and then resuspended in binding buffer [50 mM HEPES, 150 mM NaCl, 2.5 mM EGTA, 1 mM EDTA, 1 mM DTT, 0.1 mM PMSF, NP40 1% (v/v) and protease inhibitor cocktail tablets (Roche); pH 7.5]. After cells were lysed by homogenization with sonication, the insoluble material was removed by centrifugation, and the supernatant was collected as cell lysate. The cell lysate (3 mg of protein) was then incubated with XN beads (20 μL) for 3 h at 4 °C. The reacted beads were washed with binding buffer, and the binding proteins were eluted with SDS-PAGE sample buffer, separated by SDS-PAGE, and visualized by CBB staining. Identification of the proteins was performed using MALDI-TOF-MS and LC–MS/MS as previously described.[49]

***In Vitro* XN Beads Pull-Down Assay.** GST fusion proteins, which were expressed in the *Escherichia coli* BL21 strain and purified using Glutathione Sepharose 4B (GE Healthcare UK Ltd.), were incubated with XN beads in 1 mL of binding buffer for 3 h. The beads were washed with binding buffer and eluted with SDS-PAGE sample buffer. The eluted proteins were then subjected to SDS-PAGE. For the competition assay, each compound was added 1 h before incubation with XN beads.

RNA Interference. siRNA double-stranded oligonucleotides designed to interfere with the expression of VCP (sense 5′-UAGAACAGAACUCCCUUGGAAGGUG-3′; Invitrogen) and non-coding siRNA (Invitrogen) as a negative control were used. Reverse transfection was demonstrated by using HiPerFect (QIAGEN) according to the manufacturer's instructions. Briefly, A431 cells were trypsinized, resuspended in antibiotic-free medium, mixed with OPTI-MEM (Gibco) including siRNA and HiPerFect, and then seeded onto a 12-well plate. 72 h after transfection, cells were observed under microscope and lysed for Western blotting.

■ ASSOCIATED CONTENT

Accession Codes

Uni-Prot accession codes are described as following; valosion-containg protein (TERA_HUMAN), P55072; voltage-dependent anion channel (VDAC1_HUMAN), P21796; Prohibitin 2 (PHB2_HUMAN), Q99623; Prohibitin (PHB_HUMAN), P35232

■ AUTHOR INFORMATION

Corresponding Author

*E-mail: imoto@bio.keio.ac.jp.

Author Contributions

#These authors contributed equally to this work.

Notes

The authors declare no competing financial interest.

■ ACKNOWLEDGMENTS

We thank K. Honda (RIKEN, Japan) for preparing XN-beads; H. Kondo (RIKEN, Japan) for identification of XN-binding protein; S. Saiki (Juntendo University, Japan), M. Ueki, Y. Futamura, T. Saito (RIKEN, Japan) and S. Shinjo (Keio University, Japan) for technical advice; Kikkoman Corporation for kindly providing us with naringenin chalcone. We are very grateful for a grant from Hayashi Memorial Foundation for Female Natural Scientists and a scholarship from Suntory Institute for Bioorganic Research. This work was supported by a Grant-in-Aid for Scientific Research (B) and JSPS Fellows, the Ministry of Education, Culture, Sports, Science, and Technology,

■ REFERENCES

(1) Ohsumi, Y. (2001) Molecular dissection of autophagy: two ubiquitin-like systems. *Nat. Rev. Mol. Cell Biol. 2*, 211–216.

(2) Yoshimori, T. (2004) Autophagy: a regulated bulk degradation process inside cells. *Biochem. Biophys. Res. Commun. 313*, 453–458.

(3) Martinez-Vicente, M., Talloczy, Z., Wong, E., Tang, G., Koga, H., Kaushik, S., de Vries, R., Arias, E., Harris, S., Sulzer, D., and Cuervo, A. M. (2010) Cargo recognition failure is responsible for inefficient autophagy in Huntington's disease. *Nat. Neurosci. 13*, 567–576.

(4) Matsuda, N., and Tanaka, K. (2009) Does impairment of the ubiquitin-proteasome system or the autophagy-lysosome pathway predispose individuals to neurodegenerative disorders such as Parkinson's disease? *J. Alzheimer's Dis. 19*, 1–9.

(5) Mathew, R., Karantza-Wadsworth, V., and White, E. (2007) Role of autophagy in cancer. *Nat. Rev. Cancer 7*, 961–967.

(6) Ebato, C., Uchida, T., Arakawa, M., Komatsu, M., Ueno, T., Komiya, K., Azuma, K., Hirose, T., Tanaka, K., Kominami, E., Kawamori, R., Fujitani, Y., and Watada, H. (2008) Autophagy is important in islet homeostasis and compensatory increase of beta cell mass in response to high-fat diet. *Cell Metab. 8*, 325–332.

(7) Tsukada, M., and Ohsumi, Y. (1993) Isolation and characterization of autophagy-defective mutants of *Saccharomyces cerevisiae*. *FEBS Lett. 333*, 169–174.

(8) Klionsky, D. J., Cregg, J. M., Dunn, W. A. Jr., Emr, S. D., Sakai, Y., Sandoval, I. V., Sibirny, A., Subramani, S., Thumm, M., Veenhuis, M., and Ohsumi, Y. (2003) A unified nomenclature for yeast autophagy-related genes. *Dev. Cell 5*, 539–545.

(9) Lum, J. J., DeBerardinis, R. J., and Thompson, C. B. (2005) Autophagy in metazoans: cell survival in the land of plenty. *Nat. Rev. Mol. Cell Biol. 6*, 439–448.

(10) Blommaart, E. F., Krause, U., Schellens, J. P., Vreeling-Sindelarova, H., and Meijer, A. J. (1997) The phosphatidylinositol 3-kinase inhibitors wortmannin and LY294002 inhibit autophagy in isolated rat hepatocytes. *Eur. J. Biochem. 243*, 240–246.

(11) Power, B. F. B., Tutin, F., and Rogerson, H. (1913) CXXXV. The constituents of Hops. *J. Chem. Soc., Trans. 103*, 1267–1292.

(12) Tabata, N., Ito, M., Tomoda, H., and Omura, S. (1997) Xanthohumols, diacylglycerol acyltransferase inhibitors, from *Humulus lupulus*. *Phytochemistry 46*, 683–687.

(13) Inokoshi, J., Kawamoto, K., Takagi, Y., Matsuhama, M., Omura, S., and Tomoda, H. (2009) Expression of two human acyl-CoA:diacylglycerol acyltransferase isozymes in yeast and selectivity of microbial inhibitors toward the isozymes. *J Antibiot. (Tokyo) 62*, 51–54.

(14) Gerhauser, C., Alt, A., Heiss, E., Gamal-Eldeen, A., Klimo, K., Knauft, J., Neumann, I., Scherf, H. R., Frank, N., Bartsch, H., and Becker, H. (2002) Cancer chemopreventive activity of xanthohumol, a natural product derived from hop. *Mol. Cancer Ther. 1*, 959–969.

(15) Albini, A., Dell'Eva, R., Vene, R., Ferrari, N., Buhler, D. R., Noonan, D. M., and Fassina, G. (2006) Mechanisms of the antiangiogenic activity by the hop flavonoid xanthohumol: NF-kappaB and Akt as targets. *FASEB J. 20*, 527–529.

(16) Lust, S., Vanhoecke, B., Van Gele, M., Boelens, J., Van Melckebeke, H., Kaileh, M., Vanden Berghe, W., Haegeman, G., Philippe, J., Bracke, M., and Offner, F. (2009) Xanthohumol activates the proapoptotic arm of the unfolded protein response in chronic lymphocytic leukemia. *Anticancer Res. 29*, 3797–3805.

(17) Kabeya, Y., Mizushima, N., Ueno, T., Yamamoto, A., Kirisako, T., Noda, T., Kominami, E., Ohsumi, Y., and Yoshimori, T. (2000) LC3, a mammalian homologue of yeast Apg8p, is localized in autophagosome membranes after processing. *EMBO J. 19*, 5720–5728.

(18) Yamamoto, A., Tagawa, Y., Yoshimori, T., Moriyama, Y., Masaki, R., and Tashiro, Y. (1998) Bafilomycin A1 prevents maturation of autophagic vacuoles by inhibiting fusion between autophagosomes and lysosomes in rat hepatoma cell line, H-4-II-E cells. *Cell Struct. Funct. 23*, 33–42.

(19) Vigneswaran, N., Wu, J., Song, A., Annapragada, A., and Zacharias, W. (2011) Hypoxia-induced autophagic response is associated with aggressive phenotype and elevated incidence of metastasis in orthotopic immunocompetent murine models of head and neck squamous cell carcinomas (HNSCC). *Exp. Mol. Pathol. 90*, 215–225.

(20) Kanoh, N., Honda, K., Simizu, S., Muroi, M., and Osada, H. (2005) Photo-cross-linked small-molecule affinity matrix for facilitating forward and reverse chemical genetics. *Angew. Chem., Int. Ed.. 44*, 3559–3562.

(21) Ju, J. S., Fuentealba, R. A., Miller, S. E., Jackson, E., Piwnica-Worms, D., Baloh, R. H., and Weihl, C. C. (2009) Valosin-containing protein (VCP) is required for autophagy and is disrupted in VCP disease. *J. Cell Biol. 187*, 875–888.

(22) Tresse, E., Salomons, F. A., Vesa, J., Bott, L. C., Kimonis, V., Yao, T. P., Dantuma, N. P., and Taylor, J. P. (2010) VCP/p97 is essential for maturation of ubiquitin-containing autophagosomes and this function is impaired by mutations that cause IBMPFD. *Autophagy 6*, 217–227.

(23) Ye, Y., Meyer, H. H., and Rapoport, T. A. (2001) The AAA ATPase Cdc48/p97 and its partners transport proteins from the ER into the cytosol. *Nature 414*, 652–656.

(24) Jarosch, E., Taxis, C., Volkwein, C., Bordallo, J., Finley, D., Wolf, D. H., and Sommer, T. (2002) Protein dislocation from the ER requires polyubiquitination and the AAA-ATPase Cdc48. *Nat. Cell Biol. 4*, 134–139.

(25) Mouysset, J., Deichsel, A., Moser, S., Hoege, C., Hyman, A. A., Gartner, A., and Hoppe, T. (2008) Cell cycle progression requires the CDC-48UFD-1/NPL-4 complex for efficient DNA replication. *Proc. Natl. Acad. Sci. U.S.A. 105*, 12879–12884.

(26) Partridge, J. J., Lopreiato, J. O. Jr., Latterich, M., and Indig, F. E. (2003) DNA damage modulates nucleolar interaction of the Werner protein with the AAA ATPase p97/VCP. *Mol. Biol. Cell 14*, 4221–4229.

(27) Rouiller, I., DeLaBarre, B., May, A. P., Weis, W. I., Brunger, A. T., Milligan, R. A., and Wilson-Kubalek, E. M. (2002) Conformational changes of the multifunction p97 AAA ATPase during its ATPase cycle. *Nat. Struct. Biol. 9*, 950–957.

(28) DeLaBarre, B., and Brunger, A. T. (2003) Complete structure of p97/valosin-containing protein reveals communication between nucleotide domains. *Nat. Struct. Biol. 10*, 856–863.

(29) Song, C., Wang, Q., and Li, C. C. (2003) ATPase activity of p97-valosin-containing protein (VCP). D2 mediates the major enzyme activity, and D1 contributes to the heat-induced activity. *J. Biol. Chem. 278*, 3648–3655.

(30) Wang, Q., Song, C., and Li, C. C. (2003) Hexamerization of p97-VCP is promoted by ATP binding to the D1 domain and required for ATPase and biological activities. *Biochem. Biophys. Res. Commun. 300*, 253–260.

(31) Wang, Q., Song, C., Yang, X., and Li, C. C. (2003) D1 ring is stable and nucleotide-independent, whereas D2 ring undergoes major conformational changes during the ATPase cycle of p97-VCP. *J. Biol. Chem. 278*, 32784–32793.

(32) Yamanaka, K., Sasagawa, Y., and Ogura, T. (2012) Recent advances in p97/VCP/Cdc48 cellular functions. *Biochim. Biophys. Acta 1823*, 130–137.

(33) Wojcik, C., Rowicka, M., Kudlicki, A., Nowis, D., McConnell, E., Kujawa, M., and DeMartino, G. N. (2006) Valosin-containing protein (p97) is a regulator of endoplasmic reticulum stress and of the degradation of N-end rule and ubiquitin-fusion degradation pathway substrates in mammalian cells. *Mol. Biol. Cell 17*, 4606–4618.

(34) Hirabayashi, M., Inoue, K., Tanaka, K., Nakadate, K., Ohsawa, Y., Kamei, Y., Popiel, A. H., Sinohara, A., Iwamatsu, A., Kimura, Y., Uchiyama, Y., Hori, S., and Kakizuka, A. (2001) VCP/p97 in abnormal protein aggregates, cytoplasmic vacuoles, and cell death, phenotypes relevant to neurodegeneration. *Cell Death Differ. 8*, 977–984.

(35) Kobayashi, T., Tanaka, K., Inoue, K., and Kakizuka, A. (2002) Functional ATPase activity of p97/valosin-containing protein (VCP) is required for the quality control of endoplasmic reticulum in neuronally differentiated mammalian PC12 cells. *J. Biol. Chem. 277*, 47358–47365.

(36) Gao, X., Deeb, D., Liu, Y., Gautam, S., Dulchavsky, S. A., and Gautam, S. C. (2009) Immunomodulatory activity of xanthohumol: inhibition of T cell proliferation, cell-mediated cytotoxicity and Th1 cytokine production through suppression of NF-kappaB. *Immunopharmacol. Immunotoxicol. 31*, 477–484.

(37) Pan, L., Becker, H., and Gerhauser, C. (2005) Xanthohumol induces apoptosis in cultured 40–16 human colon cancer cells by activation of the death receptor- and mitochondrial pathway. *Mol. Nutr. Food Res. 49*, 837–843.

(38) Deeb, D., Gao, X., Jiang, H., Arbab, A. S., Dulchavsky, S. A., and Gautam, S. C. (2010) Growth inhibitory and apoptosis-inducing effects of xanthohumol, a prenylated chalone present in hops, in human prostate cancer cells. *Anticancer Res. 30*, 3333–3339.

(39) Dai, R. M., Chen, E., Longo, D. L., Gorbea, C. M., and Li, C. C. (1998) Involvement of valosin-containing protein, an ATPase Co-purified with IkappaBalpha and 26 S proteasome, in ubiquitin-proteasome-mediated degradation of IkappaBalpha. *J. Biol. Chem. 273*, 3562–3573.

(40) Asai, T., Tomita, Y., Nakatsuka, S., Hoshida, Y., Myoui, A., Yoshikawa, H., and Aozasa, K. (2002) VCP (p97) regulates NFkappaB signaling pathway, which is important for metastasis of osteosarcoma cell line. *Jpn. J. Cancer Res. 93*, 296–304.

(41) Yamamoto, S., Tomita, Y., Hoshida, Y., Takiguchi, S., Fujiwara, Y., Yasuda, T., Yano, M., Nakamori, S., Sakon, M., Monden, M., and Aozasa, K. (2003) Expression level of valosin-containing protein is strongly associated with progression and prognosis of gastric carcinoma. *J. Clin. Oncol. 21*, 2537–2544.

(42) Yamamoto, S., Tomita, Y., Uruno, T., Hoshida, Y., Qiu, Y., Iizuka, N., Nakamichi, I., Miyauchi, A., and Aozasa, K. (2005) Increased expression of valosin-containing protein (p97) is correlated with disease recurrence in follicular thyroid cancer. *Ann. Surg. Oncol. 12*, 925–934.

(43) Bursavich, M. G., Parker, D. P., Willardsen, J. A., Gao, Z. H., Davis, T., Ostanin, K., Robinson, R., Peterson, A., Cimbora, D. M., Zhu, J. F., and Richards, B. (2010) 2-Anilino-4-aryl-1,3-thiazole inhibitors of valosin-containing protein (VCP or p97). *Bioorg. Med. Chem. Lett. 20*, 1677–1679.

(44) Chou, T. F., and Deshaies, R. J. (2011) Quantitative cell-based protein degradation assays to identify and classify drugs that target the ubiquitin-proteasome system. *J. Biol. Chem. 286*, 16546–16554.

(45) Chou, T. F., Brown, S. J., Minond, D., Nordin, B. E., Li, K., Jones, A. C., Chase, P., Porubsky, P. R., Stoltz, B. M., Schoenen, F. J., Patricelli, M. P., Hodder, P., Rosen, H., and Deshaies, R. J. (2011) Reversible inhibitor of p97, DBeQ, impairs both ubiquitin-dependent and autophagic protein clearance pathways. *Proc. Natl. Acad. Sci. U.S.A. 108*, 4834–4839.

(46) Wang, Q., Shinkre, B. A., Lee, J. G., Weniger, M. A., Liu, Y., Chen, W., Wiestner, A., Trenkle, W. C., and Ye, Y. (2010) The ERAD inhibitor Eeyarestatin I is a bifunctional compound with a membrane-binding domain and a p97/VCP inhibitory group. *PLoS One 5*, e15479.

(47) Balgi, A. D., Fonseca, B. D., Donohue, E., Tsang, T. C., Lajoie, P., Proud, C. G., Nabi, I. R., and Roberge, M. (2009) Screen for chemical modulators of autophagy reveals novel therapeutic inhibitors of mTORC1 signaling. *PLoS One 4*, e7124.

(48) Saiki, S., Sasazawa, Y., Imamichi, Y., Kawajiri, S., Fujimaki, T., Tanida, I., Kobayashi, H., Sato, F., Sato, S., Ishikawa, K., Imoto, M., and Hattori, N. (2011) Caffeine induces apoptosis by enhancement of autophagy via PI3K/Akt/mTOR/p70S6K inhibition. *Autophagy 7*, 176–187.

(49) Kawatani, M., Okumura, H., Honda, K., Kanoh, N., Muroi, M., Dohmae, N., Takami, M., Kitagawa, M., Futamura, Y., Imoto, M., and

Osada, H. (2008) The identification of an osteoclastogenesis inhibitor through the inhibition of glyoxalase I. *Proc. Natl. Acad. Sci. U.S.A. 105*, 11691−11696.

dx.doi.org/10.1021/cb200492h | *ACS Chem. Biol.* XXXX, XXX, XXX−XXX